International Journal of Precision Engineering and Manufacturing (2026) 27:403–437
https://doi.org/10.1007/s12541-025-01370-y

Online ISSN 2005-4602
Print ISSN 2234-7593

REVIEW PAPER

# Recent Advancements in Filtration Technique for Engineering Surface Topography using High-Definition Metrology

**Yiping Shao[1] · Zhilong Xu[1] · Shichang Du[2] · Jiansha Lu[1]**

Received: 8 August 2025 / Revised: 23 September 2025 / Accepted: 28 September 2025 / Published online: 31 October 2025


**Abstract**

Breakthroughs in high-definition metrology have propelled the characterization of engineering surface topography from qualitative description to quantitative analysis. Surface topography filtration, as a core technology for separating multi-scale features, has seen its methodological innovations and application expansions become a critical demand in precision manufacturing and advanced materials. This paper systematically reviews the evolution of engineering surface topography filtration technology: from traditional linear methods to nonlinear multiscale analysis techniques, to geometry-aware filtering, and finally to cutting-edge methods driven by artificial intelligence. It reveals a progressive paradigm shift from "noise suppression" to "feature enhancement" and "function awareness". For typical engineering surfaces, including continuous flat, multi-hole discontinuous, and freeform surfaces, this paper presents a comparative analysis of the application scenarios and inherent limitations of various filtering methods. It focuses on the breakthrough progress of artificial intelligence in automating boundary detection, intelligently generating rough surfaces, and enhancing model interpretability. The study indicates that the field currently faces several core challenges in cross-scale feature characterization, computational efficiency, standardization, and mapping mechanisms for topography and function. Looking ahead, the field will focus on the deep integration of physical mechanisms with eXplainable artificial intelligence (XAI) and advanced data models. The ultimate aim is to establish reliable quantitative relationships between topography and function, thereby evolving filtration technology from a passive post-processing tool into a core enabling technology that supports predictable design and controllable manufacturing.

**Keywords** Engineering surface filtration · High-definition metrology · Geometry-aware filtering · Artificial intelligence · Surface topography

## 1 Introduction

In modern engineering science, the three-dimensional microstructure of a material's surface, known as its surface topography, is no longer regarded as a mere geometric attribute but is recognized as a critical physical parameter that dictates the final function and performance of a product [1, 2]. As schematically illustrated in Fig. 1, the topography of a real surface, which represents the actual boundary of an object, is understood as a composite of deviations from its ideal, nominal surface. Furthermore, these deviations are formally categorized into three principal components: form error, surface texture, and flaws [3, 4]. Each of these components has distinct origins and functional implications [5, 6]. Form error refers to the widely spaced deviations of the real surface from the nominal surface, such as out-of-flatness or out-of-roundness, which are typically caused

This paper is an invited paper.

✉ Shichang Du
lovbin@sjtu.edu.cn

Yiping Shao
syp123gh@zjut.edu.cn

Zhilong Xu
xzl@zjut.edu.cn

Jiansha Lu
ljs@zjut.edu.cn

[1] College of Mechanical Engineering, Zhejiang University of Technology, Hangzhou 310023, China

[2] School of Mechanical Engineering, Shanghai Jiao Tong University, Shanghai 200240, China

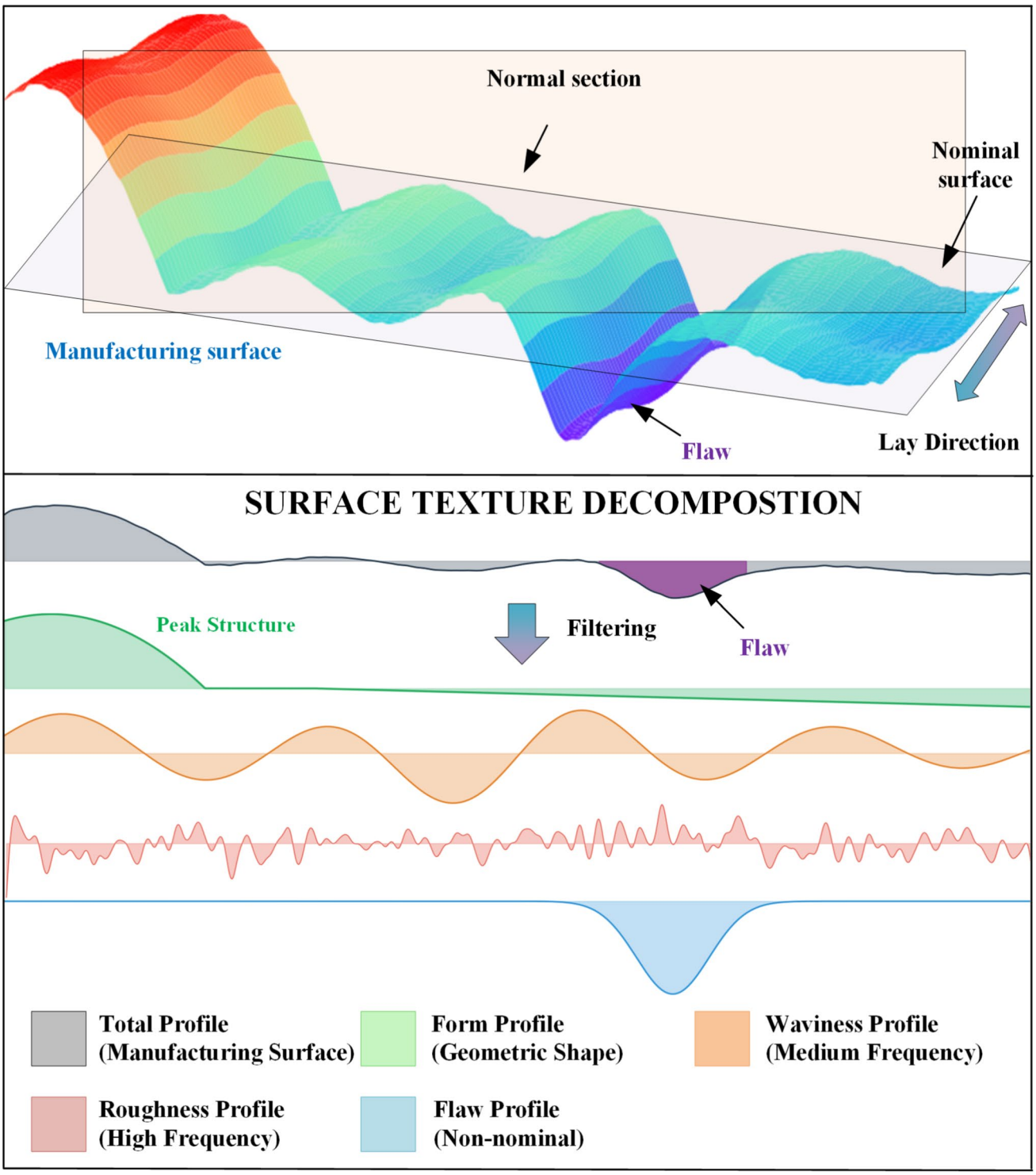


**Fig. 1** Schematic diagram of surface characteristics

by inaccuracies in the machine tool or insecure workpiece clamping. Surface texture is the composite of more finely spaced irregularities and is further decomposed into waviness and roughness, which are typically generated by the cutting tool action or machine vibrations [7]. However, flaws are distinct from both form and texture. It typically involves localized interruptions in the typical topography, such as cracks or pores, which can act as severe stress concentrators that compromise a component's fatigue life and structural integrity [8]. Therefore, it is important to detect

even micro-scale defects as their progression can lead to catastrophic failures [9, 10]. This has led to a growing emphasis on integrative multi-parameter measurement philosophies, aiming to bridge the gap between geometric metrology and defect characterization. This trend is exemplified by recent advancements in non-destructive testing and evaluation (NDT&E), where novel sensor systems are being developed to perform simultaneous measurement of geometric parameters and defects from a single data source [11, 12].

Unlike discrete flaws, surface texture is a feature that is typically ubiquitous across the entire surface, treated as a continuous, stochastic, or pseudo-periodic field. This multiscale texture, which comprises the more widely spaced waviness and the finer spaced roughness, fundamentally governs distributed functional properties such as friction, lubrication, and wear [13, 14]. Furthermore, the robust characterization of the underlying texture is often a prerequisite for reliable flaw detection, as the texture must first be filtered from the raw measured data to reveal anomalous topographical features. Consequently, the precise multiscale characterization of surface topography has become a central element in quality control, failure prediction, and high-performance design in frontier domains such as aerospace and automotive manufacturing, as illustrated in Fig. 2 [15–18].

The rapid development of high-definition metrology techniques, such as laser scanning [19], atomic force microscopy (AFM) [20], Coherence Scanning Interferometry (CSI) [21, 22], structured light profilometry [22, 23], and laser holographic interferometry [24], has provided an unprecedented data foundation for the aforementioned multiscale characterization [25]. However, while these technologies yield massive volumes of high-precision data, they also introduce a formidable challenge: the raw measurement data is a composite signal containing a mixture of everything from macroscopic shape to microscopic textures and even measurement noise, creating a "data-rich but information-poor" dilemma [26, 27]. Therefore, the essential task of engineering surface topography filtration is to effectively separate the feature scales relevant to specific functions from this complex composite signal and to transform the raw data into actionable knowledge, thereby bridging the "data-value gap" between immense metrology datasets and functional engineering decisions [28, 29].

The diversity of engineering surfaces further exacerbates this challenge, dictating that filtration strategies need to be highly specific. For continuous engineering surfaces, such as mechanical seal faces and precision bearing raceways, the smooth and continuous topography demands that filtration focuses on distinguishing random noise from true low-frequency waviness while preserving geometric integrity [30]. Discontinuous surfaces, such as coated substrates and additively manufactured parts with embedded features, exhibit abrupt amplitude changes like steps and peaks, requiring filters that can suppress high-frequency noise while preserving critical edge sharpness [31]. Meanwhile,

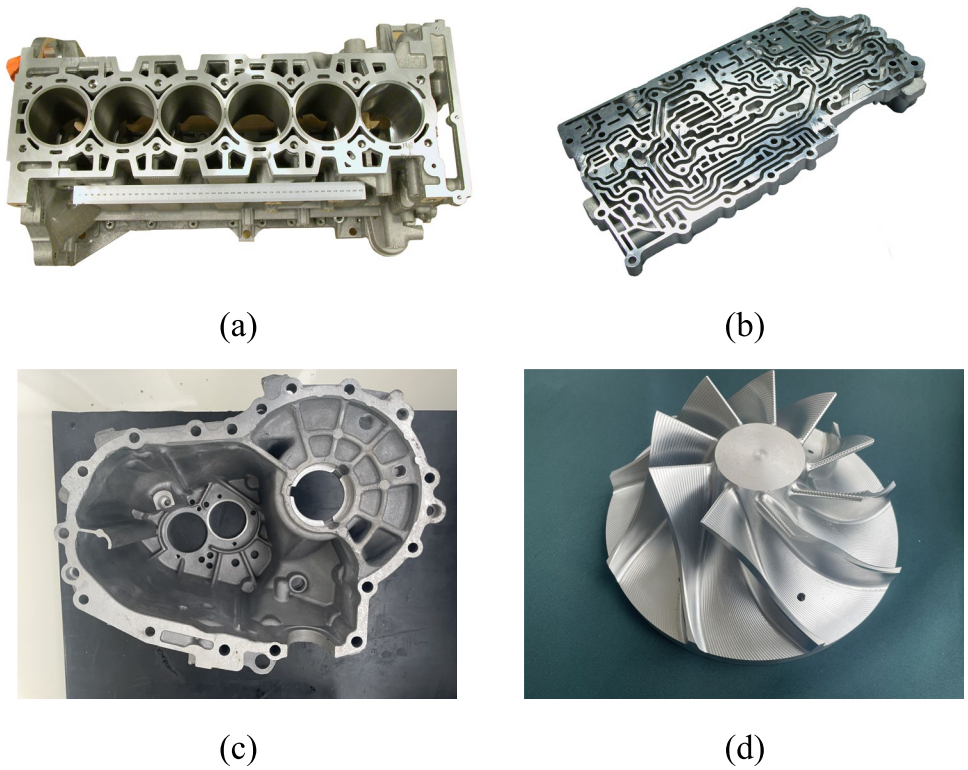


**Fig. 2** Mechanical manufacturing surface (**a**) Cylinder Block (**b**) Automatic Transmission Valve Body (**c**) Transmission Housing (**d**) Compressor Wheel

discontinuous surfaces have functional porosity or complex structures, such as engine cylinder blocks and transmission valve bodies. Their function, such as lubricant retention and sealing, is determined by multiscale networks of pores or oil grooves. Therefore, filters for these surfaces must accurately identify macroscopic geometric boundaries while resolving microscopic functional textures [32]. The specificity, driven by both surface geometry and functional requirements, has propelled filtration technology toward customized, multi-strategy development [33].

To meet these increasingly complex engineering demands, surface topography filtration technology has undergone a profound evolution from standardization to intelligence. The International Organization for Standardization (ISO) established a linear filtration framework centered on the Gaussian filter through its ISO 16610 series of standards, providing industry with a unified and traceable language for quality control [34–36]. However, the inherent time-invariant assumption of linear filters leads to edge distortion and feature blurring when processing complex surfaces with non-stationary and non-Gaussian characteristics, such as those produced by additive manufacturing or laser texturing [37]. From another perspective, this limitation has powerfully driven the evolution toward adaptive and data-driven methods. Nonlinear multiscale analysis techniques, represented by wavelet transform [38], empirical mode decomposition [39], and morphological filtration [40], achieve precise capture of local and transient features by decomposing topography into intrinsic modes or multi-scale signals [41].

When the analysis extends to freeform surfaces like turbine blades, their complex non-Euclidean geometric properties have propelled the development of geometry-aware filters based on the Laplace-Beltrami operator [42], manifold diffusion [43], and other techniques [44], which operate directly on 3D meshes to smooth noise while preserving the surface's intrinsic topological features [45]. More recently, the integration of artificial intelligence has brought revolutionary breakthroughs. Deep learning models can automate boundary detection on discontinuous surfaces [46], while generative adversarial networks (GANs) can simulate rough surfaces with specific statistical properties for algorithm validation [47–50]. It marks a paradigm shift in filtration technology from "signal and geometric processing" to "intelligent functional perception" [51].

To systematically sort out the knowledge system of the field, this paper is organized to follow the intrinsic logic of technological evolution. It begins by examining high-definition metrology technologies as the source of data and their inherent constraints on filtration algorithms. Secondly, it reviews the paradigm evolution of filtration technology from standardization to adaptivity. Building on this foundation, it provides an in-depth analysis and comparison of mainstream and advanced filtering methods for typical flat, discontinuous, and freeform surfaces. Concurrently, it offers a systematic analysis of AI applications, discussing how recent advancements like Generative Adversarial Networks (GANs), Physics-Informed Neural Networks (PINNs), and Explainable AI (XAI) provide new paradigms for solving key problems. Finally, it synthesizes these discussions to articulate the current core challenges and envisions a future research landscape focused on the deep integration of physics-informed intelligent filtration with autonomous manufacturing systems and multimodal information fusion theory. It aims to provide researchers and engineers with a reference that is both in-depth and forward-looking.

## 2 High-Definition Metrology

High-definition metrology is the source of surface topography data and constitutes the data foundation for surface integrity analysis [52]. The fidelity, resolution, and noise characteristics of this data directly determine the effectiveness and performance limits of subsequent filtration and analysis [53]. The advancement of metrology is intrinsically coupled with the escalating demands for precision and functionality in engineering, ranging from macroscopic industrial components to micro- and even nano-scale electronic structures, which perpetually drives technological innovation [54]. Figure 3 shows some of the mainstream high-definition measuring machines. However, this relationship is not unidirectional but a dynamic co-evolution. Each measurement technology, defined by its unique physical principles, inevitably imparts a distinct signature onto the data, including inherent physical limitations and measurement artifacts [55]. In turn, these intrinsic data characteristics define the specific constraints and requirements for filter design, compelling the development of tailored algorithms capable of mitigating noise and artifacts without distorting true surface features. Therefore, a comprehensive understanding of the synergistic and oppositional interplay between metrology and filtration is essential for advancing the field.

### 2.1 Contact Metrology Techniques

Contact metrology relies on the direct physical interaction between a probe and a surface to acquire topographical data. Its core advantages lie in its sub-nanometer vertical resolution and its insensitivity to the optical properties of materials, providing highly reliable data for the profile analysis of smooth, hard surfaces [56]. However, they are fundamentally limited by the mechanical convolution of the probe tip and the surface.


(a)

(b)


(c)

(d)

**Fig. 3** High-definition metrology measuring instrument (**a**) Hexagon LEITZ PMM Series (**b**) Form Talysurf CNC Series (**c**) Coherix Shapix Series (**d**) FreeScan UE Pro

Coordinate Measuring Machines (CMMs) (e.g., Hexagon LEITZ PMM series) represent the cornerstone of macro-scale contact metrology. They are designed to measure the dimensional and geometric form of components by probing discrete points in 3D space. While CMMs excel at assessing form and dimensional tolerance, they are not suited for characterizing fine-scale surface texture, which requires continuous scanning with higher-resolution probes.

Stylus Profilometers (e.g., Taylor Hobson Form Talysurf) are the classical instruments for surface texture analysis [57–59]. They achieve scanning through the continuous physical contact of a diamond probe with the surface under test. The primary limitation of this method is the "tip smoothing effect": a probe tip with a finite radius of curvature cannot perfectly replicate sharp valleys or micro-cracks, resulting in an irreversible low-pass filtering at the physical level [60]. Consequently, subsequent digital filtering does not process the "true" surface but a physically smoothed version.

This inherent loss of high-frequency information means that filtering demands are focused more on the robust suppression of random noise, such as mechanical vibration and thermal drift, rather than on the recovery of lost details [61].

Atomic Force Microscopy (AFM) extends contact metrology to the nano-scale and is the recognized standard for atomic-level resolution [62]. In its common contact or tapping modes, it acquires topography by detecting the minute forces between a sharp tip on a micro-cantilever and the sample surface. However, this extremely high resolution introduces a complex set of artifacts. These include: (1) probe-sample convolution due to the finite size of the probe, which requires correction through morphological deconvolution [63]; (2) low-frequency scanner distortion caused by the hysteresis and creep of the piezoelectric scanner, which requires shape removal through high-order polynomial fitting; and (3) high-frequency oscillatory noise from the feedback loop or environment, which requires specialized low-pass or outlier filtering for suppression [64]. Therefore, AFM data necessitates a composite filtering strategy to address these distinct, multi-source errors.

### 2.2 Non-Contact Metrology

Non-contact techniques, predominantly based on optical principles, have become mainstream due to their non-destructive, high-speed, and full-areal measurement capabilities [65]. They are especially suitable for soft, fragile, or complexly curved surfaces. However, the wave nature of light and phenomena like interference and diffraction introduce more complex artifacts compared to contact methods, placing far greater demands on the diversity and intelligence of filtering algorithms [59, 66].

Interferometry-based methods offer the highest vertical resolution. Coherence Scanning Interferometry (CSI) (e.g., Zygo NewView) achieves sub-angstrom vertical resolution by demodulating low-coherence interference fringe signals [67]. Its primary challenge arises at steep edges or discontinuities, where the superposition of light signals creates characteristic "batwing" artifacts [68]. Such artifacts are not random noise but are deterministic measurement errors strongly correlated with local geometric features. Traditional linear filters misinterpret them as real features and preserve them, leading to analytical deviations [59]. From another perspective, it has directly spurred the demand for "feature-aware" filters, requiring the development of robust algorithms or morphological filtering strategies capable of identifying and removing specific geometric artifacts.

Unlike CSI, Laser Holographic Interferometry (e.g., Coherix ShaPix series) employs highly coherent laser light, typically in a Twyman-Green configuration, to achieve large-area, high-precision measurements [24]. It is typically based on a Twyman-Green interferometer configuration and integrates two core techniques, including phase-shifting and multi-wavelength tuning, to accurately demodulate the interference signal modulated by the object's surface height. The multi-wavelength tuning technique overcomes the limited measurement range of monochromatic laser interferometry, which endows the method with the unique advantage of a centimeter-scale large depth of field at sub-micron accuracy. From a filtering perspective, the data artifacts in holographic interferometry primarily originate from the noise introduced by the coherent laser and potential registration errors that may arise when stitching multiple holograms. Therefore, in addition to requiring methods like median filtering to suppress basic noise, there are also specific demands on filtering algorithms for smoothing and ensuring consistency at the stitching boundaries.

Scanning-based optical methods acquire data point-by-point or line-by-line. Confocal Microscopy [69] and Laser Scanning [70] (e.g., Keyence LJ-G) face another class of challenges originating from optical properties. The speckle noise generated by the interaction of the laser with the material surface is a multiplicative high-frequency random noise, whose statistical properties are fundamentally different from those of Gaussian white noise [71]. Furthermore, for multi-material surfaces, variations in optical signal intensity due to different reflectivities and transparencies can directly translate into height measurement errors. It has driven the evolution of filtration algorithms from "general-purpose models" to "specialized models". For instance, denoising algorithms based on wavelet transforms or non-local means perform better against speckle noise as they are better adapted to its multiplicative statistical properties. For multi-material surfaces, intelligent filtering methods that incorporate multimodal information (such as synchronously acquired light intensity images) are required to adaptively adjust the processing strategy at the boundaries of different materials.

Structured Light Scanning technology (e.g., FreeScan UE Pro) reconstructs three-dimensional topography by projecting encoded light patterns and decoding the phase distortion, offering significant advantages in rapidly acquiring data from large freeform surfaces [52]. However, its accuracy is limited by the reliability of the phase unwrapping algorithm, which is prone to errors in areas of complex concavities or occlusions, leading to localized step-like measurement errors. These errors often manifest as outliers or regional artifacts, which place extremely high demands on the robustness of the filter. Simple linear smoothing can produce catastrophic results due to the strong influence of these outliers. Consequently, robust Gaussian regression filters, which are based on iteratively reweighted least squares, and variants of the median filter have been developed in response to this need [72].

### 2.3 The Symbiotic Evolution of Metrology and Filtration

Metrology and filtering technologies do not have a simple upstream-downstream relationship but rather a profound symbiotic evolution. As shown in Fig. 4, it reflects a logic where "algorithms adapt to the data source, and the data source drives algorithm innovation". This co-evolution represents a fundamental shift in the role of metrology and filtering, moving from a post-process, passive quality control function toward an in-process, active feedback control mechanism. Table 1 provides a summary of mainstream metrology techniques, their inherent physical limitations, and how these limitations drive the requirements for filtration algorithms.

On one hand, the physical limitations of metrology techniques are a fundamental driver of innovation in filtration algorithms [73]. The massive data volumes (on the order of billions of points) generated by high-definition, large-area measurements pose a severe challenge to the computational efficiency of filtration algorithms [73]. A complex nonlinear

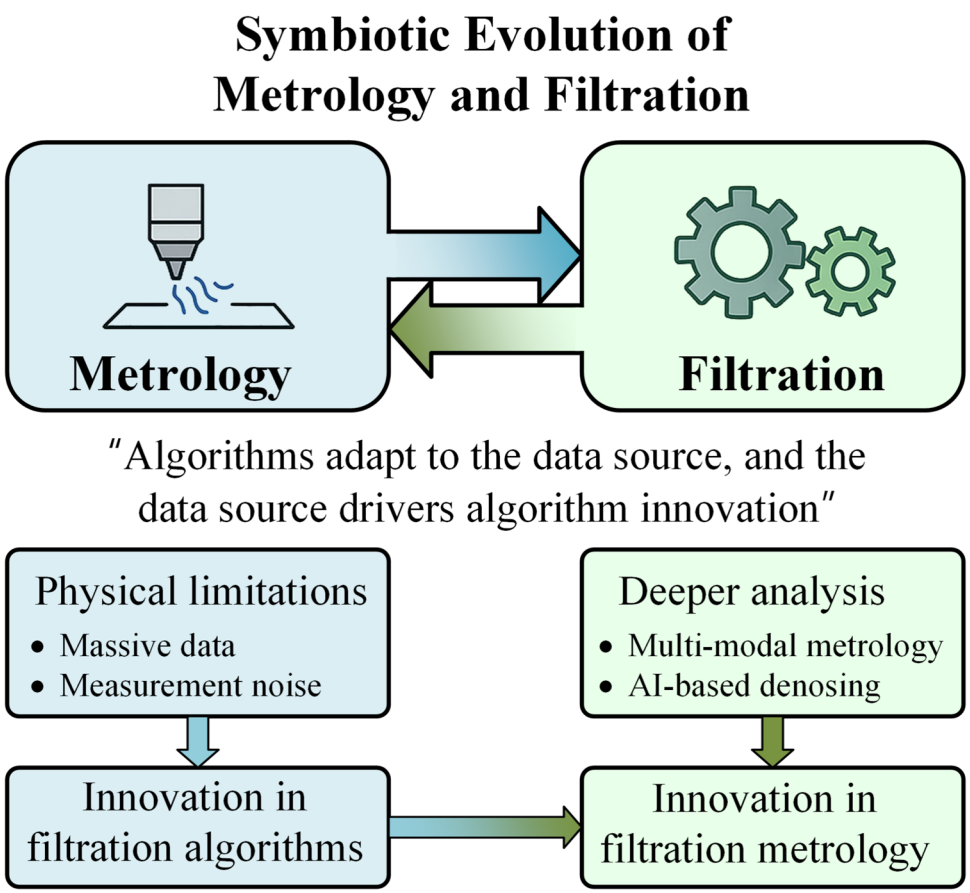


**Fig. 4** Symbiotic evolution of metrology and filtration

algorithm may perform well on a small dataset. However, its application value is greatly diminished if it cannot process the scan data of a large blade within the industrial cycle time [74]. This reality has propelled the application of technologies like parallel computing (GPU acceleration) and model order reduction techniques in the filtering domain. Furthermore, different measurement techniques introduce noise with distinct characteristics. The noise from stylus measurements may be dominated by mechanical vibrations, while the noise from optical measurements may include speckle noise and artifacts caused by non-uniform surface reflectivity [75]. Therefore, filter design must rely on prior knowledge of the specific measurement noise characteristics to achieve optimal performance, which leads to a gradual evolution from "one-size-fits-all" general-purpose models to specialized, robust, and intelligent algorithms [76].

On the other hand, the demand for deeper functional analysis drives innovation in metrology conversely, pushing it beyond purely geometric characterization. A complete understanding of a surface's functional potential requires knowledge of its material status, which encompasses localized variations in subsurface microstructure, residual stress, or chemical composition. It has spurred the development of multi-modal metrology, which integrates various sensors to provide a more holistic characterization [77, 78]. For example, techniques like eddy current testing can simultaneously assess geometric parameters (such as displacement) and differentiate materials or their properties based on electromagnetic response, effectively bridging the gap between metrology of geometry and material characterization [11, 79]. Similarly, the combination of confocal microscopy with Raman spectroscopy has the ability for the simultaneous acquisition of topography and material composition information, which can guide a filter to employ differentiated processing strategies at the boundaries of different materials [80]. This fusion of geometric and material-specific data opens new possibilities for the development of intelligent filtering algorithms that can process multi-modal information. More forward-looking research has already begun to explore embedding AI-based denoising models directly into sensor hardware to create closed-loop intelligent metrology systems that can adaptively correct measurement errors in real-time [81, 82]. In such systems, filtering is no longer an isolated post-processing step but is deeply coupled with data acquisition, together forming a complete chain from high-fidelity data acquisition to high-value information extraction [83, 84]. The ultimate goal is not just to produce a more accurate surface map, but to enable autonomous,

**Table 1** Mainstream Metrology Techniques

| Instrument | Measurement Principle | Core Advantages | Limitations | Core Demand on Filtering Algorithms |
|---|---|---|---|---|
| Contact | | | | |
| Coordinate Measuring Machine (CMM) | Probing discrete points in 3D space. | Benchmark for macro-scale form and dimensional metrology. | Not suited for fine-scale surface texture characterization. | Focus on geometric fitting rather than texture filtering. |
| Stylus Profilometer | Continuous physical scanning with a diamond probe. | Sub-nanometer vertical resolution, insensitive to optical properties. | Physical low-pass filtering: Tip radius effect causes irreversible loss of high-frequency information; Random noise: Mechanical vibration, thermal drift. | Focus on robustly suppressing random noise, rather than recovering lost high-frequency details. |
| Atomic Force Microscopy (AFM) | Detecting nano-scale forces between a sharp tip and the sample. | Atomic-level lateral and vertical resolution. | Multi-source errors: (1) Probe-sample convolution; (2) Low-frequency scanner distortion (hysteresis, creep); (3) High-frequency feedback loop noise. | Requires a composite filtering strategy: morphological deconvolution, high-order polynomial fitting, and specialized low-pass/outlier filters. |
| Non-Contact | | | | |
| Coherence Scanning Interferometry (CSI) | Demodulation of low-coherence interference fringe signals. | Sub-angstrom vertical resolution, rapid full-areal measurement. | Geometry-related artifacts: "Bat-wing" effect at steep edges; sensitive to surface slope and reflectivity changes. | Requires feature-aware morphological or robust filters capable of identifying and removing specific geometric artifacts. |
| Laser Holographic Interferometry | Coherent laser interferometry with phase-shifting and multi-wavelength tuning. | Sub-micron accuracy with large field of view and depth of field. | Coherent noise: Laser speckle; Registration errors from stitching multiple views. | Noise suppression algorithms (e.g., median filter); smoothing and consistency correction at stitching boundaries. |
| Confocal Microscopy/Laser Scanning | Laser point/line scanning to acquire data sequentially. | High speed, suitable for in-line inspection. | Multiplicative random noise: Laser speckle; Optical property errors: Variations in reflectivity; Occlusion and shadowing. | Requires specialized filters for speckle noise (e.g., wavelet, non-local means); adaptive strategies for multi-material surfaces. |
| Structured Light Scanning | Decoding distortion of projected light patterns. | Rapid data acquisition for large free-form surfaces. | Gross errors/outliers: Caused by phase unwrapping failures in occluded or complex areas. | Filters with high robustness to outliers (e.g., median filter, robust Gaussian regression). |

intelligent manufacturing systems that can self-correct and optimize in real time, connecting the technical details of filtering algorithms directly to the high-level vision of smart manufacturing [85–87].

In summary, high-definition metrology provides an unprecedentedly rich data foundation for surface topography filtration, while also bringing multifaceted challenges in terms of data scale, noise characteristics, and geometric complexity [88]. The advancement of filtration algorithms is facilitating a more precise interpretation of this complex data. The symbiotic evolution of the two fields is a key driver propelling engineering surface analysis from "geometric characterization" toward "functional prediction and control".

## 3 A Brief History of Engineering Surface Filtering

The century-long development of engineering surface filtering technology is not an isolated evolution of algorithms but a result of the synergistic drive from three forces: the functional demands of manufacturing technology, the progress of metrology science, and breakthroughs in computational power. As shown in Fig. 5, its evolutionary path clearly demonstrates a four-stage progression of the technological paradigm, shifting from simple signal separation to intelligent functional perception through a continuous interplay between "standardization" and "adaptability".

### 3.1 Stage I: The Era of Mechanical and Analog Filtering (Late 1900s–1970s)

The concept of surface filtering originated from the urgent need for precision control in mechanical processing during the Industrial Revolution. With the rise of physical stylus profilometry, early mechanical filters emerged. These filters utilized physical structures, such as mechanical levers, springs, and dampers, to smooth the movement of the stylus, thereby achieving a preliminary separation of macroscopic surface form from microscopic roughness [89]. This stage established the core idea of "separating signals based on spatial frequency (wavelength)", laying the methodological foundation for subsequent filtering theories [32, 89].

The burgeoning development of electronics in the 1940 s propelled filtering technology from purely physical

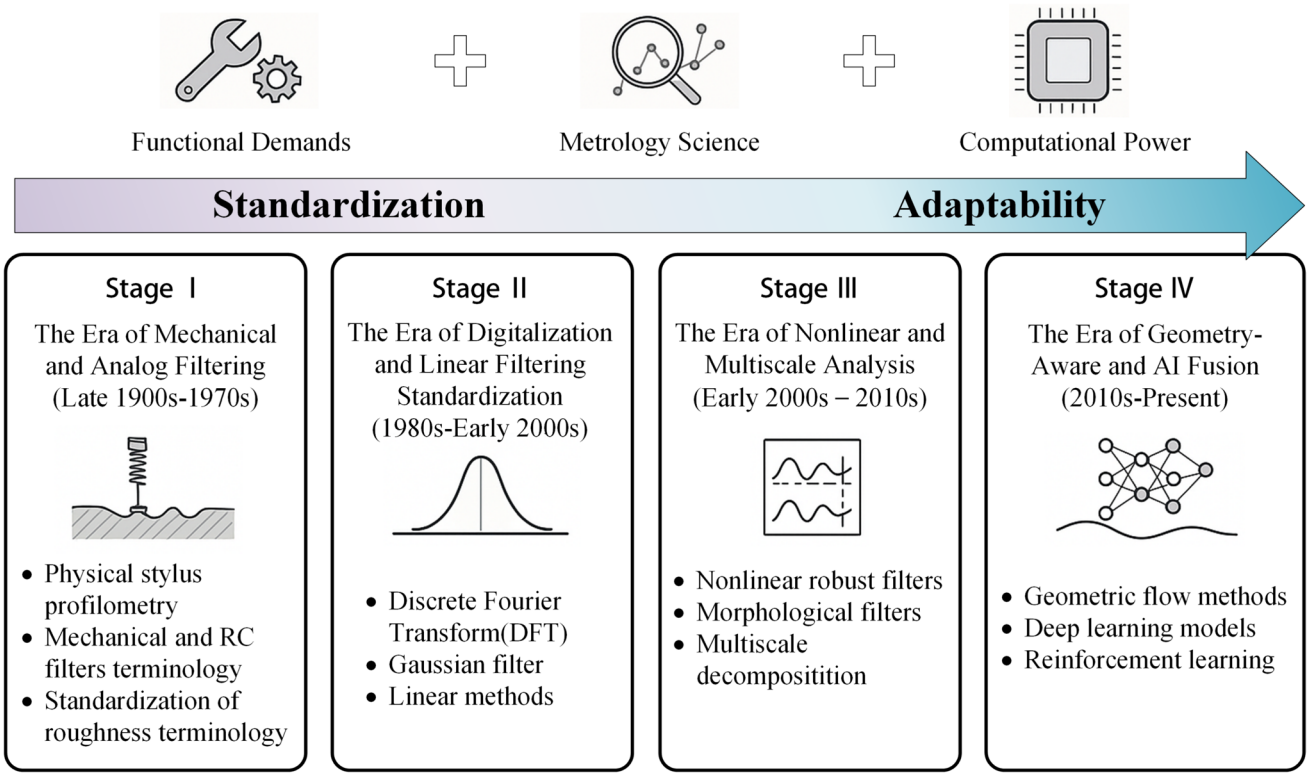


**Fig. 5** A brief history of engineering surface filtering

operations to electronic analog signal processing. Analog filters, centered on RC (resistor-capacitor) circuits, became widely used in profilometers due to their ability to perform continuous frequency-domain analysis on the electrical signals representing the surface profile. It marked the entry of filtering technology into a phase of quantitative analysis based on signal theory [36]. The publication of the ISO/R 468 standard in 1966 was a milestone of this period. It was the first to systematically standardize surface roughness terminology (such as the arithmetic mean deviation of the profile, Ra) and filtering methods (distinguishing roughness from waviness by a cutoff wavelength), which provides a unified technical language for global industrial production [58, 90]. However, the filtering characteristics of mechanical and analog filters, such as cutoff frequency, were fixed by their physical parameters, which lack the flexibility to adapt to graded textures or complex geometric surfaces. This limitation set the stage for the rise of digital methods [91].

### 3.2 Stage II: The Era of Digitalization and Linear Filtering Standardization (1980s–Early 2000 s)

The rapid advancement of computer technology and numerical algorithms allowed surface filtering to enter a critical period of digital transformation in the 1980s. The mature application of the Discrete Fourier Transform (DFT) and the Fast Fourier Transform (FFT) algorithm made it possible to perform efficient and flexible frequency-domain analysis on large-scale surface profile data [92, 93].

The central theme of this era was standardization, aimed at ensuring the comparability of surface roughness parameters across different instruments and laboratories, thereby providing a cornerstone for globalized industrial quality control. The publication of the ISO 11562 standard in 1996 was a landmark event, as it formally established the Gaussian filter as the international benchmark for surface profile filtering [94]. The Gaussian filter, based on convolution with a Gaussian kernel, possesses desirable properties such as a clear mathematical definition, high computational efficiency, and a phase-correct transfer characteristic. It quickly became the mainstream method in industry, especially for conventional surfaces with statistically isotropic features, such as automotive engine blocks and optical lenses [1, 22]. Subsequently, other linear methods like spline filtering [95] and polynomial regression [96] emerged, which to some extent improved upon the edge-blurring issues of the Gaussian filter when dealing with step boundaries. However, the linear filters of this stage were fundamentally aimed at "standardized uniformity", sacrificing the highest fidelity for complex local geometric features in exchange for a general analysis framework that was stable and produced

comparable results in the vast majority of scenarios. However, this approach also sowed the seeds of limitations for processing more complex surfaces in the future.

### 3.3 Stage III: The Era of Nonlinear and Multiscale Analysis (Early 2000s–2010s)

The rise of advanced processes such as laser surface texturing and metal additive manufacturing gave birth to complex surfaces with non-Gaussian, non-stationary, and multiscale coupled features. Their critical functions are often determined by discrete, localized microstructures with specific morphologies. In this context, the "uniform smoothing" characteristic of Linear Time-Invariant (LTI) systems like the Gaussian filter transformed from an advantage into a critical flaw, as it would blur functional peaks and blunt critical valleys, leading to a misjudgment of the surface's function [97].

To address this challenge, a revolutionary shift in the filtering paradigm occurred, formally acknowledged by the International Organization for Standardization (ISO) with the release of the ISO 16610 "Geometrical Product Specifications (GPS) – Filtration" series of standards starting in 2011. For the first time, this series elevated nonlinear and robust filters to a status equivalent to that of linear filters within the official standards system [33, 96]. Among these, the robust Gaussian regression filter (ISO 16610–31) can "ignore" outliers such as scratches and pits [72]. Morphological filters (ISO 16610–41) act directly on the surface geometry, preserving edge features through operations like erosion and dilation [98]. Concurrently, multiscale analysis methods such as the Discrete Wavelet Transform [98] (DWT) (ISO 16610–29) and Empirical Mode Decomposition [39] (EMD) upgraded filtering from a separation based on a single cutoff wavelength to an adaptive time-frequency decomposition, enabling the precise capture of directional machining textures and transient defects. The development of these technologies marked a significant shift in the filtering paradigm from a pursuit of "standardization" to a response to "adaptability".

### 3.4 Stage IV: The Era of Geometry-Aware and AI Fusion (2010s–Present)

The popularization of high-definition 3D metrology and the demand for functional analysis of complex freeform surfaces, such as aerospace turbine blades and biomimetic implants, have pushed the requirement for "adaptability" to a new dimension, propelling the deep fusion of filtering technology with computational geometry and artificial intelligence [99].

The core of geometry-aware filtering is to solve the fundamental failure of flat surface algorithms on freeform surfaces by extending the filtering operation from Euclidean space to the surface manifold [100]. Geometric flow methods, with the Laplace-Beltrami Operator (LBO) as their theoretical cornerstone, provide an intrinsic diffusion operation on the surface manifold to achieve curvature-adaptive smoothing. It perfectly generalizes the Gaussian filter to non-Euclidean spaces, ensuring the geometric consistency of the filtering process [43, 100].

The integration of artificial intelligence has provided a new, data-driven paradigm for "adaptability", where the transformation is not merely about parameter optimization but a breakthrough in methodology. Deep learning models based on architectures like U-Net can fuse global and local context to automatically identify the boundaries of multi-hole or discontinuous surfaces [101, 102]. Generative Adversarial Networks (GANs) can generate synthetic surfaces with controllable roughness characteristics to provide an efficient means for validating the performance of filtering algorithms [49, 103]. Reinforcement Learning (RL) can be used to dynamically optimize filtering parameters online, adapting to the layer-by-layer variations in surface features during manufacturing [50, 104]. Furthermore, technologies like Physics-Informed Neural Networks (PINN) and eXplainable AI (XAI) are dedicated to solving the "black box" problem of AI in engineering applications, aiming to build intelligent systems that possess both learning capabilities and physical credibility. These advancements signify that surface filtering is now entering an intelligent era driven by the "synergy of data and knowledge" [105, 106].

A core law becomes clear when looking back at this evolution: formal international standards are a lagging reflection of technological consensus, not a driver of innovation. A new technology, once validated in the research domain, becomes an established industry practice. Only after it has been widely adopted by industry and its value has been proven is it incorporated into an international standard, such as the ISO 16610 series. Currently, AI-driven filtering is in the research innovation phase and is beginning to form its own unofficial standards. The fact that ISO has initiated preliminary studies on this topic signals the beginning of its path toward formalization. This historical logic not only reveals the intrinsic driving force behind the progress of filtering technology in the continuous interplay between "standardization" and "adaptability" but also points to the future direction: the construction of hybrid frameworks that fuse the interpretability of physical models with the adaptive capabilities of AI to meet the challenges of complex engineering surfaces.

## 4 Filtering Methods in Flat Surface

Flat surfaces, being the most widespread geometric form in engineering applications, have a relatively mature system of filtering technologies. However, the technical challenges

and strategic choices within this domain are fundamentally dictated by a core property: the geometric continuity of the surface. For geometrically continuous surfaces, the central conflict in filtering lies in achieving high-fidelity separation of different signal scales (roughness, waviness, form error) while effectively suppressing noise. When the surface presents geometric discontinuities, such as pores, steps, or material interfaces, the core conflict shifts from a problem of signal fidelity to one of preserving the geometric integrity of these boundaries at the discontinuities [58, 107]. Therefore, this section discusses filtering methods for flat surfaces by categorizing them into two major scenarios: "continuous" and "discontinuous".

## 4.1 Filtering Methods for Continuous Flat Engineering Surfaces

For continuous surfaces formed by processes, such as precision grinding and polishing, stringent requirements are placed on geometric accuracy [108]. For such surfaces, like precision-ground mechanical seal faces or optical flat substrates, the filtering objective is to precisely separate mid-frequency waviness and low-frequency form error while effectively suppressing high-frequency measurement noise, and to preserve sharp edges at the boundaries of functional areas [109].

### 4.1.1 Linear Filtering Techniques

Linear filtering techniques are based on the core principle of frequency-domain separation. They achieve a hierarchical division of different wavelength components by convolving a predefined mathematical model (i.e., the filter kernel) with the surface data. The stability, computational efficiency, and well-established standardization system of these algorithms have made them a long-relied-upon fundamental method in industry [109].

(a) Gaussian Filter

As the benchmark method for linear filtering, the Gaussian filter is specified in the ISO 16610–21 and ISO 16610–61 standards and is currently the most widely used reference filter [32, 33, 110]. The filtering principle of the Gaussian filter mainly involves convolving a Gaussian weighting function with the surface topography to be processed. The profile Gaussian weighting function $S(x)$ and its transfer characteristic $A_{output}/A_{input}$ are given as follows:

$$S(x) = \frac{1}{\alpha\lambda_c}\exp\left(-\pi\left(\frac{x}{\alpha\lambda_c}\right)^2\right) \tag{1}$$

$$\frac{A_{output}}{A_{input}} = \exp\left(-\pi\left(\alpha\frac{\lambda_c}{\lambda}\right)^2\right) \tag{2}$$

The areal Gaussian weighting function $S(x,y)$ and its transfer characteristic $A_{output}/A_{input}$ are given as follows:

$$S(x,y) = \frac{1}{\alpha^2\lambda_{xc}\lambda_{yc}}\exp\left(-\pi\left(\left(\frac{x}{\alpha\lambda_{xc}}\right)^2 + \left(\frac{y}{\alpha\lambda_{yc}}\right)^2\right)\right) \tag{3}$$

$$\frac{A_{outout}}{A_{input}} = \exp\left(-\pi\left(\left(\alpha\frac{\lambda_{xc}}{\lambda}\right)^2 + \left(\alpha\frac{\lambda_{yc}}{\lambda}\right)^2\right)\right) \tag{4}$$

The filtering process of the Gaussian filter is as follows:

$$\mathrm{W} = \mathrm{Z} * \mathrm{S} \tag{5}$$

where **Z** is the surface topography to be processed, **S** is the Gaussian weighting function, **W** is the filtered surface topography, $*$ denotes the convolution operation, $\lambda_c$ represents the cutoff wavelength, and $\alpha$ is a constant such that $\alpha = \sqrt{\ln 2/\pi} = 0.4697$, which ensures that the amplitude transmission at wavelength $\lambda_c$ is 50%.

However, its fundamental limitation is that as a Linear Time-Invariant (LTI) system, it cannot adapt to local variations in the signal. When processing surfaces containing non-stationary features, such as spikes or scratches, it inevitably leads to blurring and distortion of these features. Furthermore, its inherent end effect, which is the convolution distortion caused by missing data at the boundaries, severely affects the accuracy in the boundary regions [111].

(b) Spline Filter

The Spline Filter, specified in ISO 16610–22, is an important alternative proposed to address the end effect [110, 112]. It fits the surface with piecewise polynomial functions and considers natural boundary conditions, greatly reducing boundary distortion. For an open profile, its filtering equation is:

$$[\mathrm{I} + \mu\mathrm{Q}]\,\mathrm{W} = \mathrm{Z} \tag{6}$$

where **Z** is the original profile, **W** is the filtered surface topography, **I** is the identity matrix, and **Q** is a five-diagonal symmetric matrix that depends on the sampling interval $\Delta x$ and the tension parameter $\lambda_c$, which $\mu$ relates to the cutoff wavelength.

The spline filter can better preserve the sharpness of step edges and has better form-following capability, offering higher geometric fidelity than the Gaussian filter. However, its computational complexity is relatively high, and it is

sensitive to the selection of knots, facing efficiency challenges when processing very large surface datasets [110].

While the ISO 16610 series provide a unified evaluation framework for these linear techniques, their shared reliance on linear system assumptions limits their applicability to inherently nonlinear and non-stationary complex surfaces, thereby driving the development of nonlinear multiscale analysis methods.

#### 4.1.2 Nonlinear Multiscale Analysis Methods

As the functional requirements for engineering surfaces have become more complex, the limitations of traditional linear filtering in handling non-stationary signals and coupled multiscale features have grown more pronounced. Nonlinear multiscale analysis methods have emerged in response. They rely on mathematical transformations or data-driven models to transcend the constraints of the linear system superposition principle and achieve adaptive separation of surface features [1, 109].

(a) Robust and Morphological Filtering

These two types of methods aim to solve the problems of linear filters being sensitive to outliers and unable to recognize geometric morphology. The Robust Gaussian Regression Filter (ISO 16610–31) employs an iterative reweighted least squares method to dynamically reduce the weight of anomalous points (such as scratches or pits), which allows it to "ignore" these outliers and accurately extract the underlying topography [37, 113]. The Morphological Filter (ISO 16610–41) provides a geometry-based nonlinear analysis paradigm [114, 115]. Its core lies in two fundamental operations, erosion and dilation, which use a predefined "structuring element", such as a virtual sphere, to geometrically probe the surface [116]. By combining these two operations, powerful filters can be constructed. For instance, an "opening" operation (erosion followed by dilation) can effectively remove small peak noise, while a "closing" operation (dilation followed by erosion) can fill small holes, which shows excellent performance in specific applications such as pore segmentation and MEMS surface leveling [117].

(b) Wavelet and Shearlet Transform

Wavelet and Shearlet Transforms mark a significant evolution in surface filtering. Wavelet Transform [118] (ISO 16610–29) shifted the field from separation based on a single cutoff wavelength to a true multiscale decomposition. With its multiresolution analysis capability, the wavelet transform can decompose a signal into detail and approximation components at various scales, enabling the precise capture of local and transient signal features [119, 120]. However, standard wavelets are not optimal for capturing and representing two-dimensional features with directionality, such as machining marks. As an evolution of the wavelet transform, the Shearlet Transform is a multiscale geometric analysis tool capable of providing a sparse representation of anisotropic features. Through unique shearing and anisotropic scaling operations, it can construct basis functions that are localized in arbitrary directions and at various scales, thereby achieving an optimal sparse representation of anisotropic features.

Du et al. [121] applied shearlet theory to engineering surface filtering, proposing a surface separation method based on the Non-subsampled Shearlet Transform (NSST). The core contribution of this work is the use of NSST's translation invariance and high directional sensitivity to overcome two major bottlenecks of traditional methods. Firstly, it completely avoids the severe "end effects" produced by the Gaussian filter at data boundaries. Secondly, compared to standard wavelets, it can more accurately capture and separate directional textures with distinct machining marks. The framework is shown in Fig. 6. In this method, the original surface is decomposed into sub-band coefficients of different scales and directions. These coefficients are then reorganized according to the cutoff wavelength and reconstructed via an inverse transform to finally obtain roughness, waviness, and form components with clear physical meaning.

This study demonstrated through an instance analysis of an engine cylinder head surface that the NSST filtering method not only effectively separates the surface components but also calculates surface parameters (such as Sa, Sq) that show good consistency with the results from the ISO standard Gaussian filter, ensuring compatibility with existing standards. The results, shown in Fig. 7, intuitively demonstrate the superiority of NSST over the Gaussian filter in handling boundaries; the mean surface obtained by the former is complete and without distortion, whereas the latter shows significant distortion at the boundaries.

(c) Empirical Mode Decomposition

The shearlet transform pushed model-based signal representation theory to new heights, achieving optimal sparse representation of anisotropic features through elegant mathematical design. However, when the complexity of the surface topography exceeds the descriptive capacity of any preset mathematical model, for instance, when the signal exhibits high non-stationarity and non-linearity without a clear geometric structure, a more radical adaptive analysis paradigm becomes necessary [122]. Empirical Mode Decomposition (EMD) [123] is a fully data-driven, adaptive decomposition method that does not require any pre-set

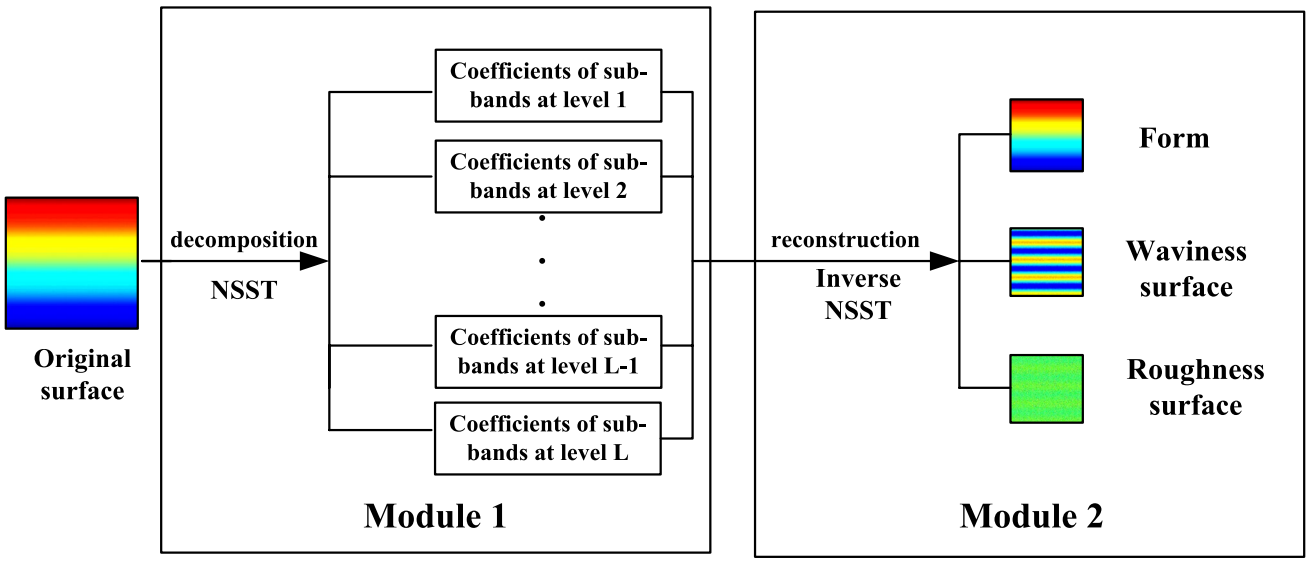


**Fig. 6** The architecture of the proposed 3 d surface separation method

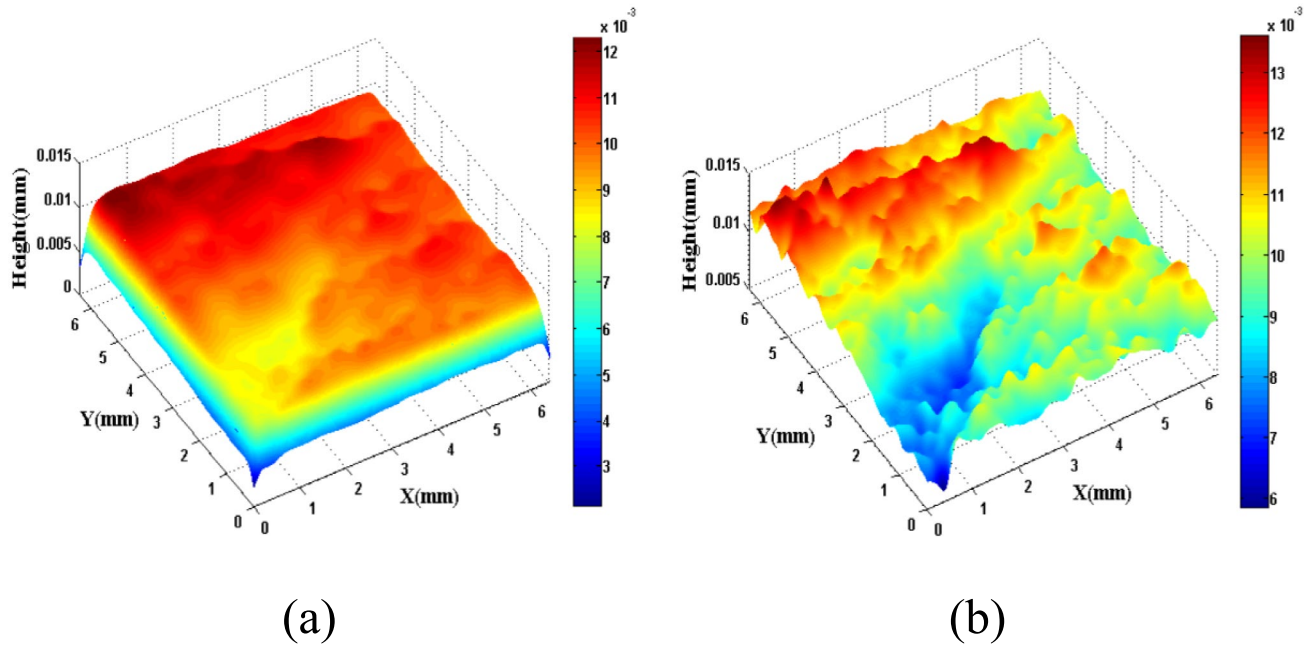


**Fig. 7** Comparison of mean surfaces results (**a**) Mean surface with Gaussian filter (**b**) Mean surface with shearlet filter

basis functions. Instead, it decomposes a complex, non-stationary, and nonlinear profile into a series of Intrinsic Mode Functions (IMFs) through a "sifting" process based on the signal's own local extrema. However, traditional EMD is hampered by two major bottlenecks: low computational efficiency and mode mixing [124].

To address these issues, Du et al. [125] proposed a Fast and Adaptive Bi-dimensional Empirical Mode Decomposition (FABEMD) method, specifically designed for processing engineering surface data from high-definition metrology. The core contribution of this work lies in introducing an adaptive windowing algorithm to automatically select the optimal filtering window size and simplifying the extremum detection process. It significantly improves computational efficiency while effectively suppressing the mode-mixing problem common in traditional BEMD methods.

The study validated the effectiveness of the FABEMD method through analysis of both simulated and real workpiece surfaces. The results showed that FABEMD can accurately separate the surface into roughness, waviness, and form components, with good consistency with the results of Gaussian filtering. More importantly, it completely avoids

the boundary effects associated with Gaussian filtering. Figure 8 intuitively demonstrates its ideal decomposition performance on a simulated surface, while Fig. 9 clearly contrasts FABEMD with the Gaussian filter in processing a real workpiece surface, highlighting the absence of boundary distortion in the former versus the obvious distortion in the latter.

In engineering practice, the selection of a filtering method is a process that requires comprehensive consideration. It depends on the functional requirements of the surface, the characteristics of the measurement equipment, and the objectives of the subsequent analysis. Table 2 summarizes the basic principles, key advantages, key limitations, and main application scenarios of the major filtering methods for continuous flat engineering surface.

## 4.2 Filtering Methods for Multi-hole and Discontinuous Flat Engineering Surfaces

When a surface presents geometric discontinuities such as pores, steps, or material interfaces, the core challenge of the filtering task shifts from the fidelity of "signal separation" to the "geometric preservation" of boundaries [33, 126, 127].

The development of advanced filtering strategies for such surfaces has led to two major technical schools of thought. The first is based on an "explicit geometric constraint" strategy, which involves explicitly identifying discontinuous boundaries with an independent edge detection operator and then applying special treatment to these boundaries during the filtering process [128, 129]. The second is based on an "implicit adaptive decomposition" strategy, which does not rely on edge detection but instead uses more advanced, data-driven decomposition techniques that naturally adapt to the local discontinuities of the signal during the decomposition process [39, 130]. This philosophical divide between "explicit" and "implicit" approaches reflects two distinctly different ways of thinking when dealing with complex geometric problems.

### 4.2.1 Explicit Geometric Constraint Strategy

The core of this type of method is "first identify, then process". It involves explicitly identifying the discontinuous boundaries of the surface using an independent edge detection operator and then applying special constraints to these boundaries during the filtering process to mechanistically avoid boundary distortion [128, 129]. A representative technical path for implementing this strategy is to draw an analogy between the filtering process and the physical diffusion phenomena [43, 131]. The foundation of this approach is anisotropic diffusion filtering, which abstracts the filtering process as a heat diffusion process. By introducing a spatially varying diffusion coefficient, it allows for smoothing in flat regions while suppressing it at edges.

The work by Wang et al. [127] made a critical improvement to this method for engineering surfaces with well-defined geometric boundaries. Their core contribution was the design of an explicit edge detector based on a binary

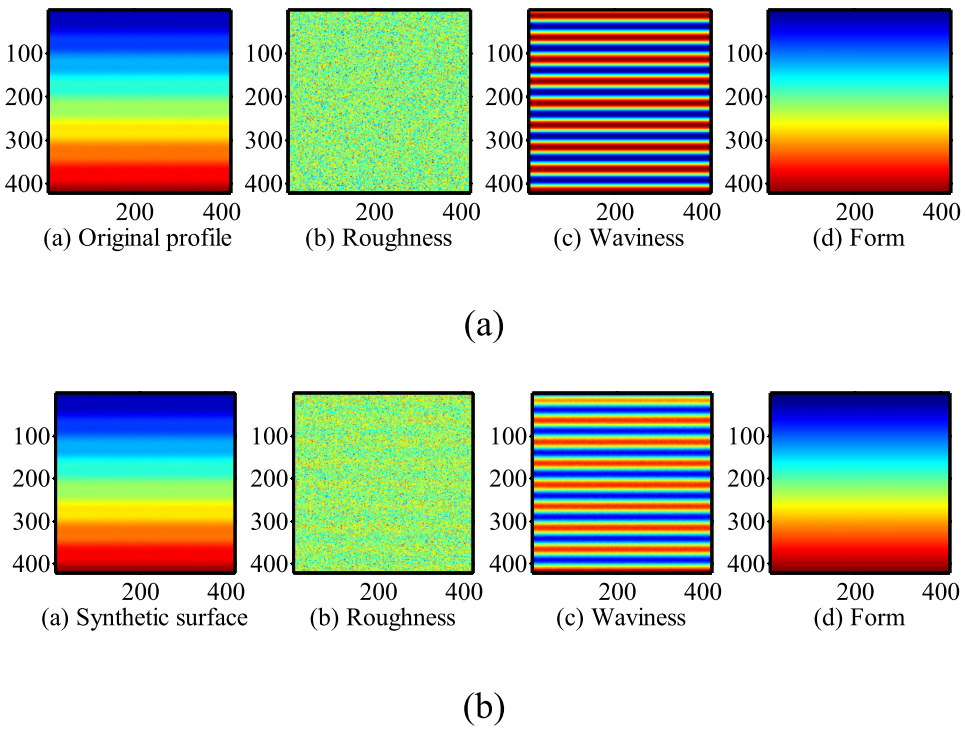


**Fig. 8** Filtering result of simulated surface using the proposed FABEMD approach (**a**) Simulated surface and its components (**b**) Filtering result

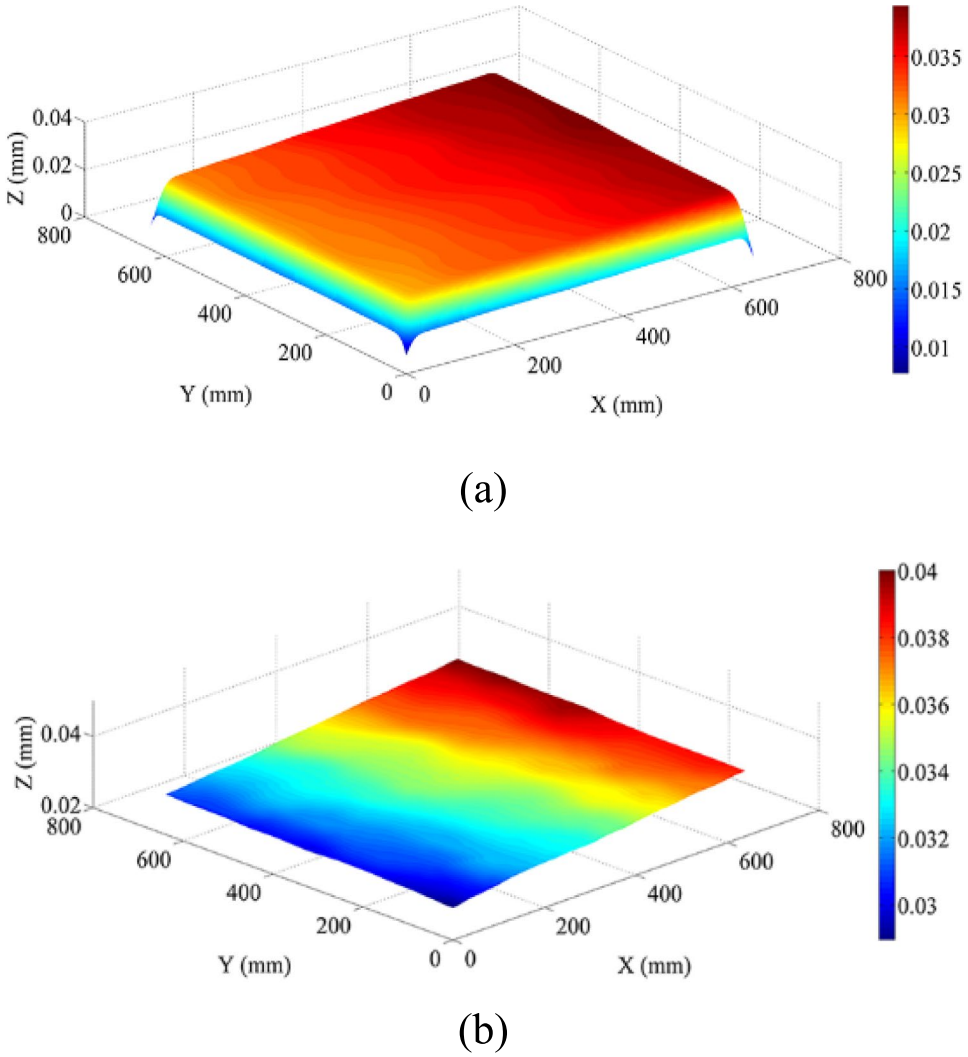


**Fig. 9** Comparison of mean surfaces obtained by the Gaussian filter and FABEMD (**a**) mean surface with Gaussian filter (**b**) mean surface of FABEMD

mask. This detector predefines the valid data points and the holes/non-measured areas on the surface, thereby constructing an "insulating wall" that algorithmically prohibits any diffusion across the geometric boundaries. This design fundamentally solves the problem of information leakage and signal distortion that occurs with traditional filters at discontinuous edges.

Furthermore, the work established a direct mathematical relationship between the diffusion time $t$ and the ISO standard Gaussian cutoff wavelength $\lambda_c$, given by $t = 0.0176\left(\frac{\lambda}{l}\right)^2$ (where $l$ is the sampling interval), ensuring the comparability of the filtering results with existing industrial standards. The effectiveness of this method was clearly verified through simulation experiments. Fig. 10 intuitively compares the processing results of a Gaussian filter and this diffusion filter on a simulated surface with a central square hole. The results show that the Gaussian filter produced severe distortion artifacts at both the inner and outer boundaries, as shown in Fig. 10(a), whereas their method perfectly separated the form and waviness components without distortion, as shown in Fig. 10(a), fully demonstrating its superiority in preserving geometric boundary integrity.

Unlike diffusion algorithms that directly control the filtering process in the spatial domain, the Tetrolet Transform integrates the idea of geometric constraints into the framework of multiscale analysis. It is an adaptive geometric wavelet transform whose basic principle is to divide an image into non-overlapping 4 × 4 pixel blocks and find the optimal "tetromino tiling" within each block to apply the Haar wavelet, thereby enabling the transform basis to conform as closely as possible to the local geometric structure of the image [132]. As shown in Fig. 11, ignoring rotations and flips, there are five different forms of tetrominoes, known as free tetrominoes. It's clear that any image of size N × N (where N is even) can be tiled by free tetrominoes.

**Table 2** Comparative analysis of the major filtering methods for continuous flat engineering surface

| Filtering Method | Basic Principle | Key Advantages | Key Limitations | Main Application Scenarios |
|---|---|---|---|---|
| Gaussian Filter (ISO 16610–21/61) | Convolution with a Gaussian kernel function to achieve low-pass filtering. | Computationally efficient, mathematically well-defined, highly standardized. | Produces blurring and distortion at discontinuities such as steps and spikes. | Routine quality control, surfaces with uniform statistical properties (e.g., ground, polished surfaces). |
| Spline Filter (ISO 16610–22) | Piecewise polynomial function fitting, ensuring derivative continuity at nodes. | Excellent edge preservation capability, no significant end effects. | Higher computational complexity, sensitive to node selection. | Surfaces with discontinuous features like steps and coating boundaries. |
| Gaussian Regression Filter (ISO 16610–31) | Iterative reweighted least squares method, reducing the weight of outliers. | Robust against outliers such as spikes and scratches. | Iterative process is time-consuming; convergence depends on initial conditions. | Surfaces containing random defects or noise spikes (e.g., EDM surfaces). |
| Morphological Filter (ISO 16610–41/81) | Based on erosion and dilation operations with a structuring element. | Suitable for nonlinear feature extraction; can identify specific geometric structures. | Sensitive to the choice of structuring element; relatively high computational load. | Pore/grain segmentation, MEMS surface leveling, probe tip deconvolution. |
| Wavelet Transform (ISO 16610–29) | Multiresolution analysis, decomposing a signal into detail and approximation components at different scales. | Excellent time-frequency localization capability; effective for extracting transient, local features. | The choice of mother wavelet and decomposition levels affects the results; lacks standardization. | Defect detection, directional texture analysis, multiscale feature separation. |
| Shearlet Transform | Multiscale geometric analysis with directional sensitivity. | Superior capability for capturing anisotropic features; can precisely characterize directional textures. | Theory and algorithms are relatively complex; high computational cost. | Surfaces with distinct machining marks (e.g., turned, milled, ground surfaces). |
| Empirical Mode Decomposition (EMD/FABEMD) | Adaptive decomposition into Intrinsic Mode Functions (IMFs) based on the signal's own characteristics. | Fully data-driven, no pre-set basis functions; suitable for non-stationary, nonlinear signals. | Prone to mode mixing and end effects; sensitive to noise. | Surfaces from multi-process manufacturing, biomedical surfaces, and function-topography correlation studies. |

Specifically, there are 117 recommended free tetromino tiling combinations.

Building on this, Shao et al. [107] proposed an extended tetrolet transform method, which is a typical representative of the "explicit geometric constraint" strategy. The core contribution of this work is a "first identify, then partition and process" filtering framework. Firstly, a specially designed edge detection operator generates a binary mask to precisely identify all boundaries and holes on a discontinuous surface. Then, guided by this mask, different transformation strategies are applied to different regions. In continuous, non-edge regions, the algorithm adaptively selects the optimal tetromino combination for transformation by minimizing the principle of sparse representation. In the identified edge regions, a specially designed, fixed Haar wavelet transform matrix is used. This "partitioned governance" strategy enables the method to effectively filter out noise in the interior regions while preserving the geometric integrity of arbitrarily shaped pores and boundaries. The study clearly demonstrated the superiority of this method through comparative simulation experiments. Figure 12 provides an intuitive comparison of the results of processing the same surface with holes using a Gaussian filter, a spline filter, and the extended tetrolet transform. Both the Gaussian and spline filters produced significant distortion artifacts at the edges of the holes, whereas the result from the extended tetrolet transform perfectly maintained the sharpness of the boundaries, proving the method's effectiveness.

#### 4.2.2 Implicit Adaptive Decomposition Strategy

This class of methods does not rely on explicit edge detection. Instead, it uses more advanced, data-driven decomposition techniques to break down the complex surface signal into a series of fundamental modes and achieves filtering by assigning physical meaning to these modes. The advantage of this approach is its holistic nature and adaptability, but its challenge lies in how to connect the abstract mathematical modes with engineering-comprehensible physical scales [133].

(a) Empirical Wavelet Transform (EWT)

Within this strategy, the Wavelet Transform is one of the most mature and fundamental techniques, providing a powerful mathematical framework for the adaptive decomposition of signals through multiresolution analysis [130].

Among these, the Biorthogonal Wavelet Transform [134] relaxes the requirement of traditional orthogonal wavelets that the analysis and synthesis filters must be

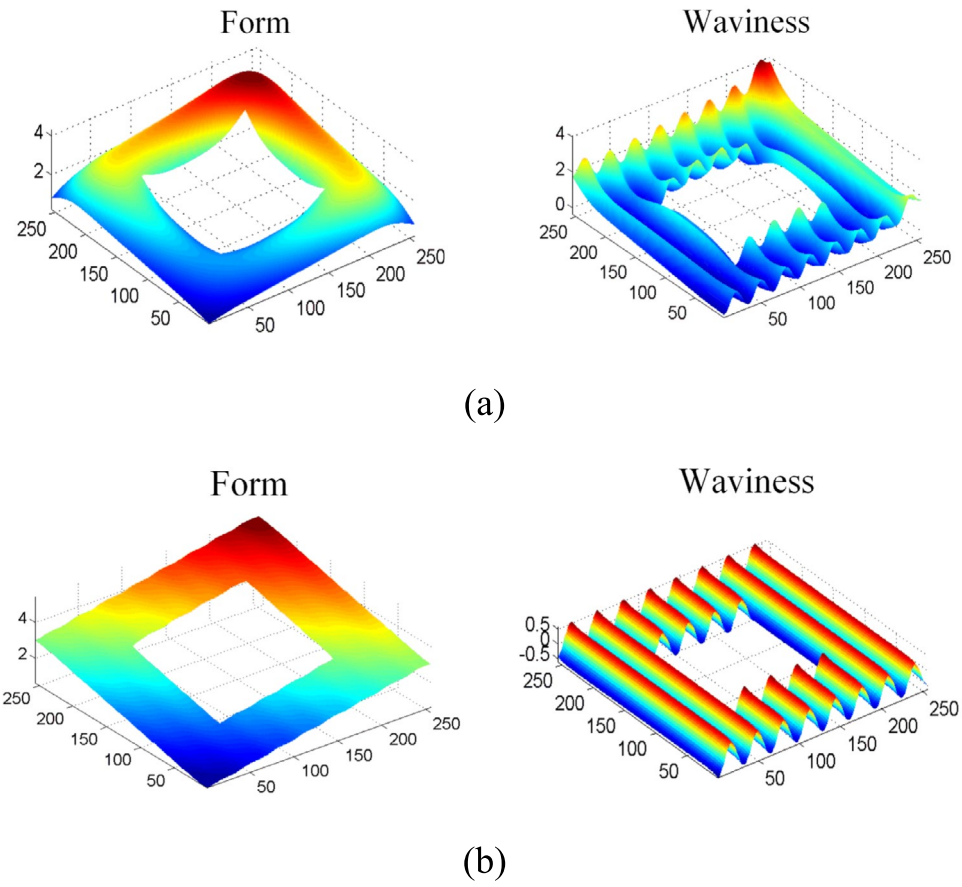


**Fig. 10** Filtered surface form and waviness (**a**) Gaussian filter (**b**) Diffusion filter

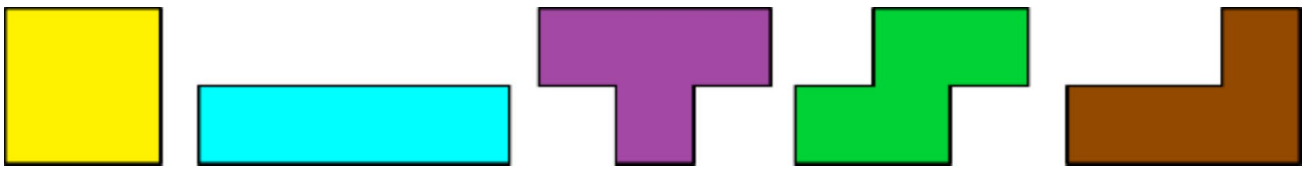

**Fig. 11** The five free tetrominoes

the same, instead using two different but related wavelets: one for decomposition (analysis wavelet) and another for reconstruction (synthesis wavelet), which performs particularly well when processing discontinuous surfaces [135]. Although the wavelet transform provides a powerful multiscale analysis framework, its performance still depends on the a priori selection of the mother wavelet. Fixed basis functions are ineffective for describing surfaces that are intrinsically complex, non-stationary, and nonlinear. To address this challenge, a more radical adaptive decomposition concept, Empirical Mode Decomposition (EMD) and its variants, provides a new solution path [39]. It requires no preset basis functions and instead decomposes a complex non-stationary, nonlinear profile into a series of Intrinsic Mode Functions (IMFs) through a "sifting" process based on the signal's own local extrema. However, traditional EMD suffers from low computational efficiency, mode mixing, and a lack of a solid mathematical foundation [136, 137].

To address these issues, a hybrid method that fuses the adaptivity of EMD with the theoretical rigor of wavelet transforms, the Empirical Wavelet Transform (EWT), was developed [138, 139]. Building on this, Shao et al. [140] further proposed an Extended Bi-dimensional Empirical Wavelet Transform (EBEWT) specifically for engineering surfaces. The method first adaptively segments the Fourier spectrum based on engineering surface data acquired via High-Definition Metrology (HDM), using polynomial fitting and scale-space representation to define the frequency boundaries for different "empirical modes". Then, based on these adaptively determined boundaries, the algorithm constructs a customized wavelet filter bank to decompose the original surface

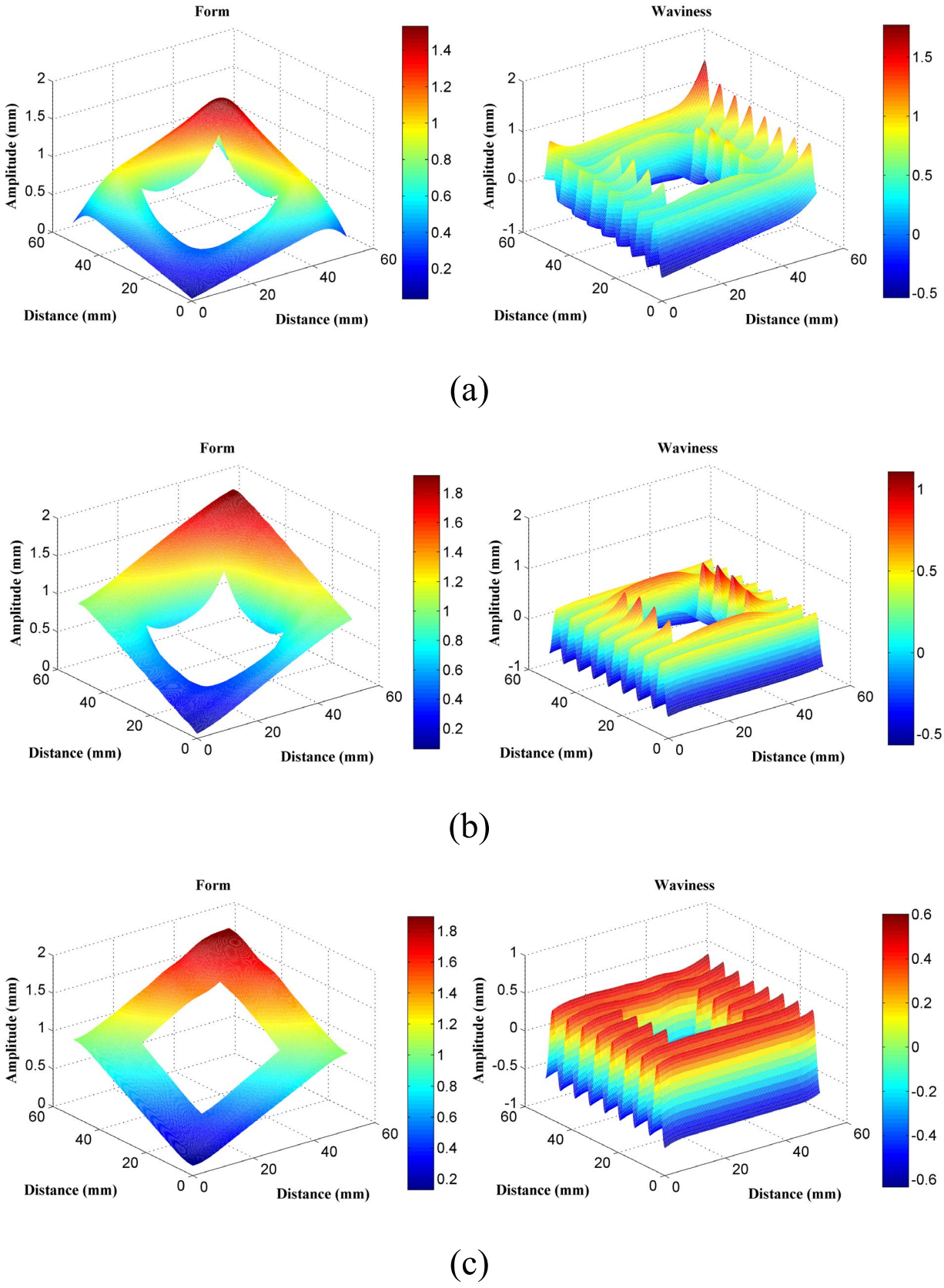


**Fig. 12** Comparison of the results (**a**) Results of areal Gaussian filter (**b**) Results of areal spline filter (**c**) Results of the extended tetrolet transform

into a series of IMFs with compactly supported frequency bands, effectively avoiding the mode mixing problem of traditional EMD. Finally, using the Riesz transform, a clear physical wavelength is calculated for each decomposed IMF. It allows the modes to be reconstructed according to the cut-off wavelengths defined in ISO standards, ultimately yielding shape, waviness, and roughness components with clear physical meaning. This complete process of "first adaptive decomposition, then physical mapping" successfully builds a bridge between data-driven adaptability and the standardization of engineering applications (i.e., separation based on wavelength). The study clearly demonstrated its effectiveness through simulation experiments. Figure 13 provides an intuitive comparison of the filtering results from the original BEWT method and the EBEWT method on the same simulated surface. As shown, the original BEWT, due to mode mixing, resulted in a separated waviness component that contained a large amount of roughness information, whereas EBEWT successfully separated the three components (form, waviness, roughness) cleanly, showing high agreement with the theoretical ground truth.

(b) Discrete Modal Decomposition (DMD)

Discrete Modal Decomposition (DMD) offers a completely new filtering perspective derived from structural dynamics and system theory [141, 142]. Unlike traditional signal processing methods, it treats the measured two-dimensional surface topography as a "snapshot" of a complex spatial dynamical system at a particular moment. The goal is to decompose the surface into a series of orthogonal "dynamic modes" by solving for a low-rank linear operator that describes the spatial evolution of the system's modes. However, these abstract modes derived from a mathematical model lack a clear physical scale and cannot be directly mapped with the engineering-defined components such as roughness and waviness.

To solve this fundamental problem, Shao et al. [143] proposed the Extended Discrete Modal Decomposition (EDMD) method. The core contribution of this work is the introduction of the two-dimensional Hilbert transform to assign an equivalent physical wavelength to each abstract "dynamic mode" extracted from the finite element modal analysis. This innovative "physical scale mapping" step successfully builds a bridge between system identification theory and surface metrology standards, making it possible to recombine different modes according to ISO cutoff wavelengths to separate the standard surface components. Figure 14 shows some of the mode shapes resulting from a modal analysis of a 30 mm × 30 mm square surface with fixed boundaries.

The unique advantage of the EDMD method lies in its excellent performance in processing discontinuous surfaces. Comparative experiments showed that, compared to Gaussian filtering, robust Gaussian regression filtering, spline filtering, and the extended tetrolet transform, EDMD was the only method that could produce clear, distortion-free filtering results. All other methods produced varying degrees of distortion artifacts at the boundaries of the holes. Furthermore, the various parameter errors of EDMD

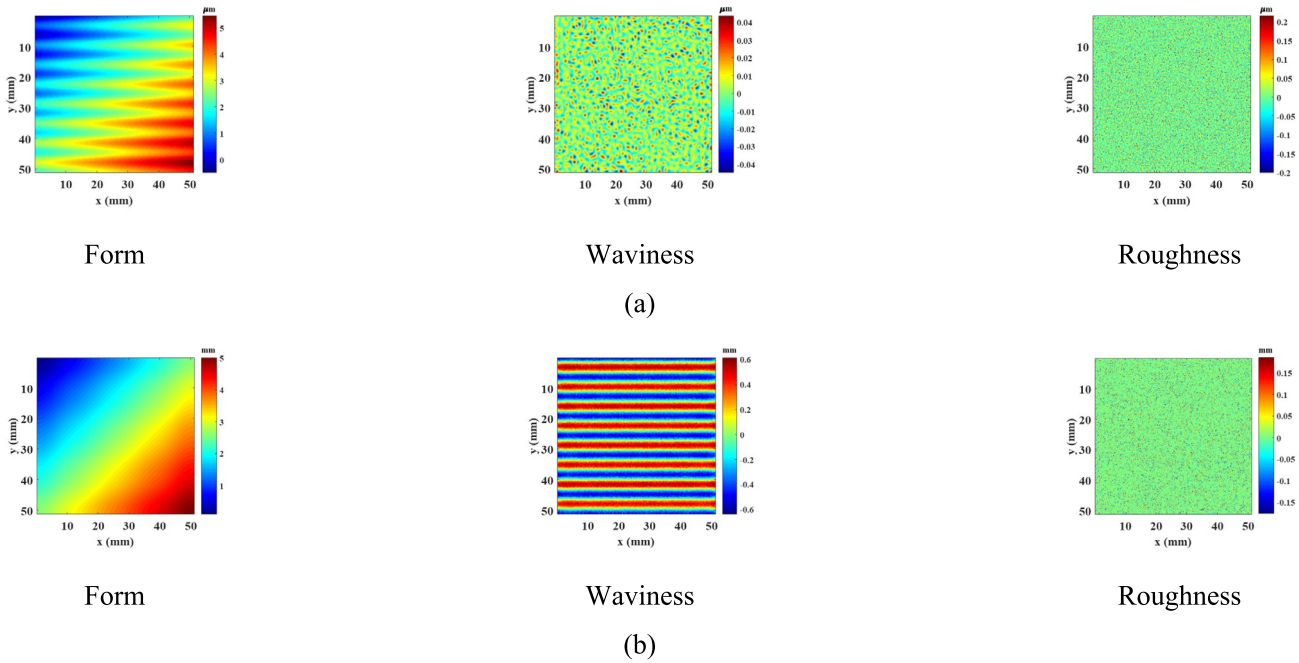


**Fig. 13** Filtering results of forms, waviness and roughness (a) The original BEWT (b) EBEWT

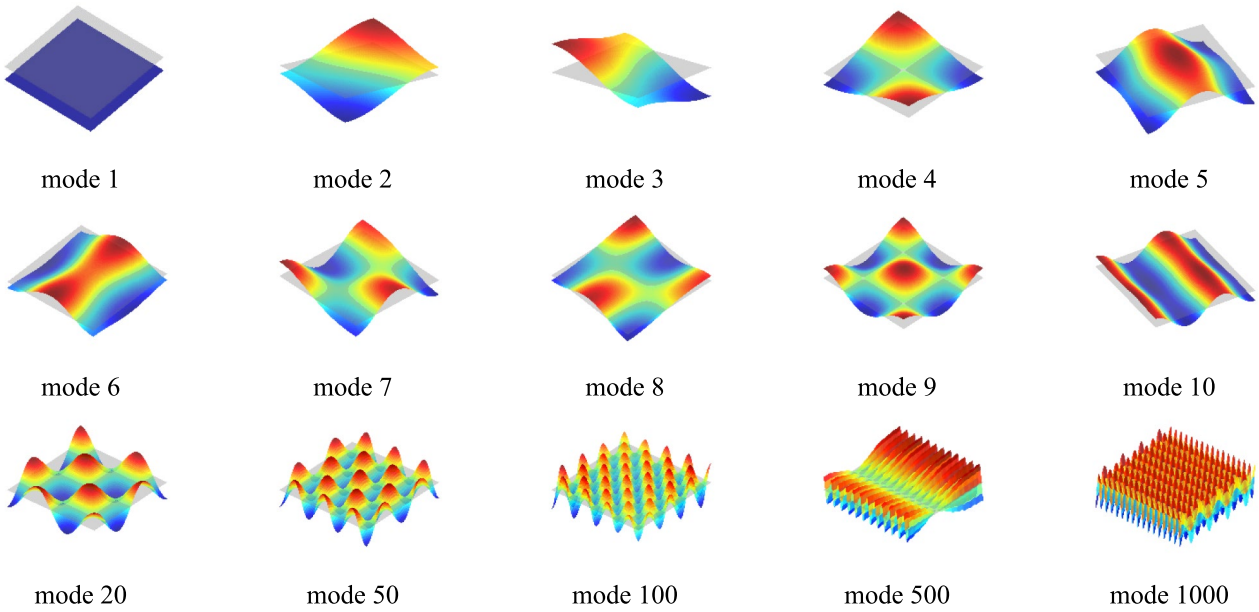


**Fig. 14** Modal basis Q of a square surface

were significantly lower than those of the other compared methods.

### 4.3 Summary

Filtering of flat and discontinuous surfaces addresses the core challenge of decomposing complex topographies into functionally relevant scales. This section reviews the evolution of techniques, from traditional linear filters, such as Gaussian and spline methods characterized by fixed cutoff wavelengths, to adaptive multiscale analysis approaches, including Wavelet Transform and Empirical Mode Decomposition (EMD). It marks a critical paradigm shift from simple "smoothing" to "adaptive feature separation", which enables a more physically interpretable characterization of non-stationary surfaces. For discontinuous surfaces, such as those with multi-hole networks, the emphasis shifts to robust boundary handling and preservation of feature integrity. However, these methods were primarily developed for Euclidean domains. When applied to freeform surfaces where curvature and topology dominate, inherent limitations emerged. The shortcoming necessitates the development of geometry-aware filtering techniques based in manifold theory, as discussed in the subsequent section.

## 5 Filtering Methods in Freeform Surfaces

When the object of analysis expands from flat surfaces to freeform surfaces, the complexity of surface filtering undergoes a qualitative leap. Freeform surfaces, with their non-Euclidean manifold characteristics, non-planar symmetry, and strong coupling of function and geometric form, pose fundamental challenges to surface filtering technology [144, 145].

Traditional filtering methods based on Cartesian coordinate system fail completely in this context, as their isotropic kernel functions cannot adapt to the continuously varying curvature of the surface. It leads to excessive smoothing in convex regions and insufficient smoothing in concave regions, resulting in severe feature distortion [146]. Therefore, the development of freeform surface filtering technology is intrinsically a process of deep fusion between signal processing theory and differential and computational geometry. Its technical evolution exhibits a clear hierarchy of abstraction, progressing from the construction of continuous mathematical theory to the implementation of discrete algorithms, and finally to the interpretation of functional features.

### 5.1 Geometric Flow Filtering Theory

The core challenge in extending filtering theory from Euclidean space to a freeform surface manifold lies in redefining the basic operation of "smoothing" so that it can act intrinsically and without distortion on a curved geometric body [147]. As shown in Fig. 15, geometric flow, based on partial differential equations (PDEs), provides a solution that is both mathematically rigorous and physically intuitive. It abstracts the filtering process as an evolutionary process on the surface manifold that conforms to physical laws [43, 131, 145]. The cornerstone of this theory is the

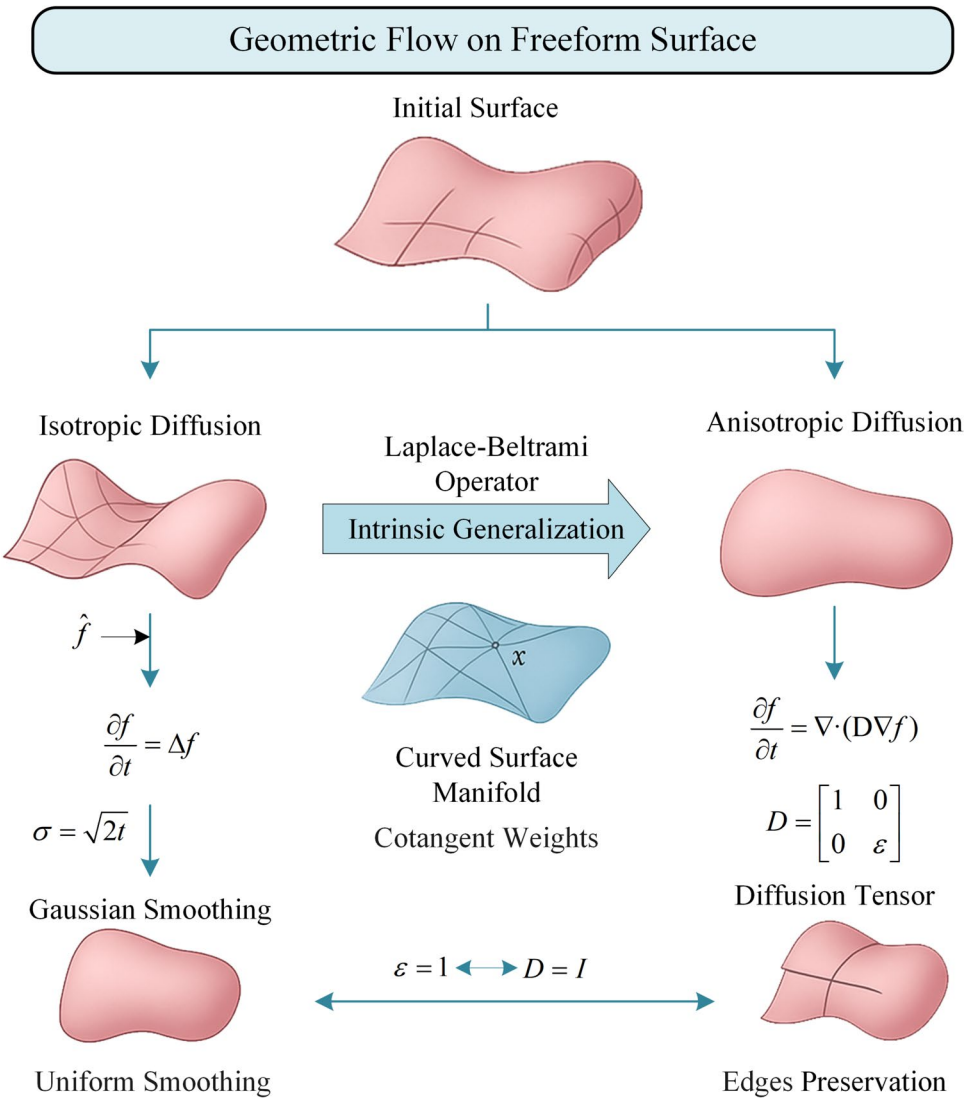


**Fig. 15** Geometric flow on free-form surface

establishment of a mathematical equivalence between the ISO standard Gaussian filter and the physical phenomenon of heat diffusion.

The pioneering work of Jiang et al. [145] pointed out that in Euclidean space, applying a Gaussian filter to a surface function $f_0$ is completely equivalent to the solution of the isotropic heat diffusion equation $f(t)$, $\frac{\partial f}{\partial t} = \Delta f$, where time $t$ controls the filtering scale (the standard deviation of the Gaussian kernel $\sigma = \sqrt{2t}$), and $\Delta$ is the standard Laplacian operator. Therefore, the key to extending Gaussian filtering to freeform surfaces is to replace the planar Laplacian operator with its unique intrinsic generalization on a Riemannian manifold, the Laplace-Beltrami Operator (LBO), denoted as $\nabla_{LB}$. The LBO is a purely intrinsic differential operator whose definition depends only on the first fundamental form (the metric tensor) of the surface and is independent of the surface's embedding in three-dimensional space or its parameterization. It fundamentally guarantees the geometric consistency and objectivity of the filtering operation [44, 148].

On a discrete triangular mesh constructed from measurement data, the LBO can be numerically approximated through the geometric relationships of a vertex's local neighborhood. The discretization scheme based on cotangent weights has become the most widely adopted approach due to its good locality, symmetric positive-definiteness, and its ability to accurately reproduce the linear function space [149]. Thus, solving the diffusion equation on a freeform surface $\frac{\partial f}{\partial t} = \nabla_{LB} f$, its solution at time $t$ is equivalent to performing a Gaussian smoothing on the initial surface $f_0$ with a scale controlled by time $t$, in a manner that completely preserves geometric consistency. The LBO not only provides a "first principles" theoretical guarantee for

performing ISO-compliant Gaussian filtering on any topological surface but also constitutes the theoretical foundation of the entire freeform surface filtering field.

However, while isotropic diffusion based on the LBO perfectly inherits the mathematical rigor of the standard Gaussian filter, it also carries over its inherent limitation. The "indiscriminate" smoothing will inevitably blunt sharp edges, directional textures, and other critical functional features while suppressing noise [150, 151]. To address this, researchers have developed Anisotropic Diffusion Filtering, whose core idea is to endow the diffusion process with "intelligent" adaptive capabilities by dynamically adjusting the smoothing intensity and direction based on local geometric information [151]. Specifically, the diffusion equation is modified $\frac{\partial f}{\partial t} = \nabla_{LB} f$ to $\frac{\partial f}{\partial t} = \nabla \cdot (\mathrm{D} \nabla f)$, where the diffusion coefficient $D$ is extended from a constant to a function or a second-order tensor that depends on local geometric features such as curvature or gradient. For example, in regions of gentle curvature change, $D$ takes a larger value to achieve Gaussian-like smoothing, while in edge regions with sharp curvature changes, $D$ approaches zero to suppress smoothing, thereby achieving a balance between noise suppression and feature preservation.

Furthermore, multi-directional free diffusion algorithms achieve more refined anisotropic control by upgrading the scalar diffusion coefficient $D$ to a second-order diffusion tensor. The eigenvectors of this tensor are aligned with the principal curvature directions of the surface, and its eigenvalues are inversely proportional to the magnitude of the principal curvatures. It allows diffusion to proceed at different rates along different directions. For example, for a surface with fine machining marks, the algorithm can enhance smoothing along the direction of the marks (to remove roughness) while weakening smoothing perpendicular to the marks (to preserve the profile features). This tensor-guided directional diffusion capability makes it highly valuable in applications such as aero-engine blades and freeform optics, where both overall surface smoothness and the preservation of microtextures are required [152].

### 5.2 Multiscale Decomposition on Discrete Meshes

After establishing the solid theoretical foundation of the LBO, the core problem for engineering applications becomes how to efficiently and stably achieve multiscale decomposition in a discrete computational environment [153, 154]. Two representative types of techniques have been developed: algebraic construction methods, represented by the lifting wavelet transform [155], and geometric iterative methods, represented by iterative mesh relaxation. These two approaches present a sharp contrast in their technical paths [156, 157].

A typical example of the algebraic construction path is the Lifting Wavelet Transform [158], which aims to construct the multiresolution framework of classical wavelets directly on irregular meshes in a purely algebraic and topological manner [159]. The work by Abdul-Rahman et al. [160] laid the foundation for this with its core idea being the decomposition of the complex wavelet transform into three reversible algebraic steps: Split (dividing the vertex set into an approximation set and a detail set), Predict (using the approximation set vertices to predict the detail set vertices to extract high-frequency information), and Update (adjusting the approximation set to maintain the conservation of low-order geometric moments). This process can be executed recursively to achieve a multiscale decomposition of the surface, as shown in Fig. 16. Its significant advantages include: (1) it is a completely in-place computation, avoiding large-scale matrix operations; (2) its computational complexity is linear concerning the number of vertices, making it highly efficient; (3) it does not require pre-processing for surface parameterization, making it applicable to any topological structures. However, the performance of this method depends on the splitting strategy and the design of the prediction and update operators. Optimizing these operators for complex scenarios, such as high-genus surfaces, remains an open research direction.

In contrast to the algebraic decomposition approach, the geometric iterative path views filtering as a process of gradual "attenuation" of high-frequency geometric energy [43, 150]. Iterative Mesh Relaxation is a typical representative of this approach [153, 160]. Its schematic diagram is shown in Fig. 17. The multiscale filtering scheme proposed by Jiang et al. [160] follows this line of thought. Its mathematical essence is an energy minimization process based on gradient descent, where high-frequency noise is preferentially attenuated because it contains higher "geometric energy" (manifested as sharp local curvature). However, traditional uniformly weighted Laplacian relaxation, while smoothing noise, indiscriminately blunts sharp edges and leads to mesh shrinkage. To address this, researchers have proposed weighted or implicit Laplacian relaxation schemes [161]. By introducing non-uniform weights related to local geometry (similar to the mechanism of anisotropic diffusion) or by solving an implicit equation to resist shrinkage, a better balance between noise suppression and feature preservation can be achieved. Although this method is conceptually intuitive and has a good analogy with the physical annealing process, its theoretical rigor is relatively insufficient. A core obstacle to its standardized application in engineering metrology is the challenge of precisely establishing an

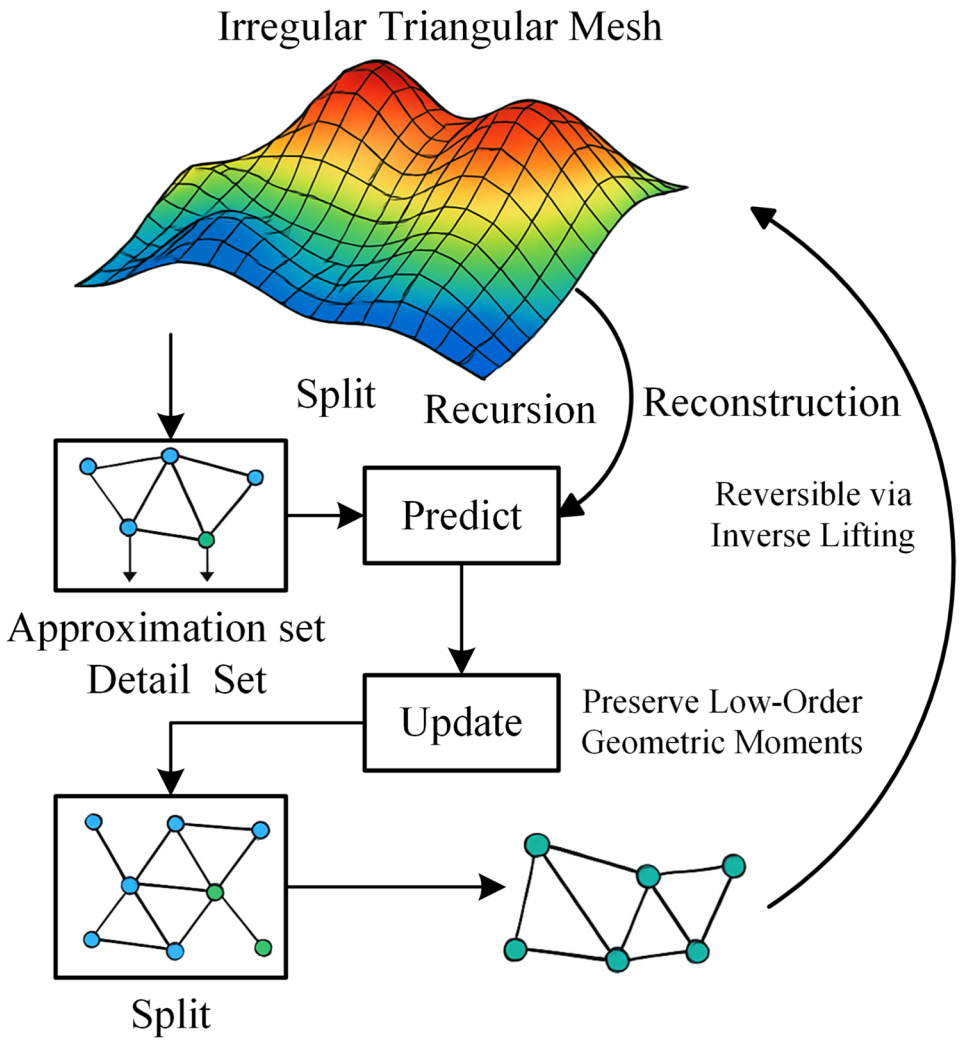


**Fig. 16** Lifting wavelet transform

analytical correspondence between the number of iterations and an ISO standard cutoff wavelength [1].

### 5.3 Surface Feature Segmentation and Quantification

Once multiscale decomposition of the surface topography has been achieved through filtering, a more advanced analytical objective is to identify, segment, and quantify discrete topographical features that have a direct impact on the part's performance from the functionally relevant textured surfaces, such as roughness and waviness components. It marks a cognitive upgrade in the analysis task, moving from processing a continuous "scale" field to identifying discrete "feature" objects [1, 162]. This shift from a scale-based analysis to a feature-based one is crucial for establishing a more direct and powerful link between topography and function. Researchers have introduced advanced theories from computational geometry and topological analysis into surface metrology, forming two complementary technical solutions.

The first is the watershed segmentation algorithm, which is based on topology and Morse theory [163]. It provides a systematic solution for the complete and non-overlapping partitioning of feature regions on freeform surfaces [164]. Lou et al. [165] rigorously extended the watershed algorithm from image processing to 3D freeform surfaces. Its theoretical foundation is discrete Morse theory [166], which provides a strict topological framework for analyzing gradient flow and critical points on discrete triangular meshes. As shown in Fig. 18. The algorithm proceeds as follows: firstly, it identifies all critical points on the surface (local minima or "pits", local maxima or "peaks", and saddle points or "passes") through topological analysis. Then, it simulates an "immersion" process of geodesic expansion starting from the bottom of the "pits" to construct a discrete gradient flow field. When the expansion regions from different "pits" meet, the boundary line is defined as a "ridge

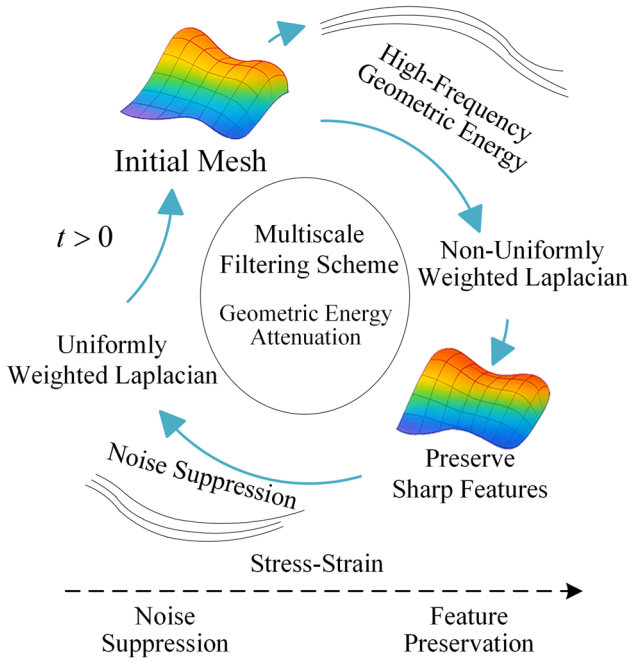


**Fig. 17** Iterative mesh relaxation for feature preservation

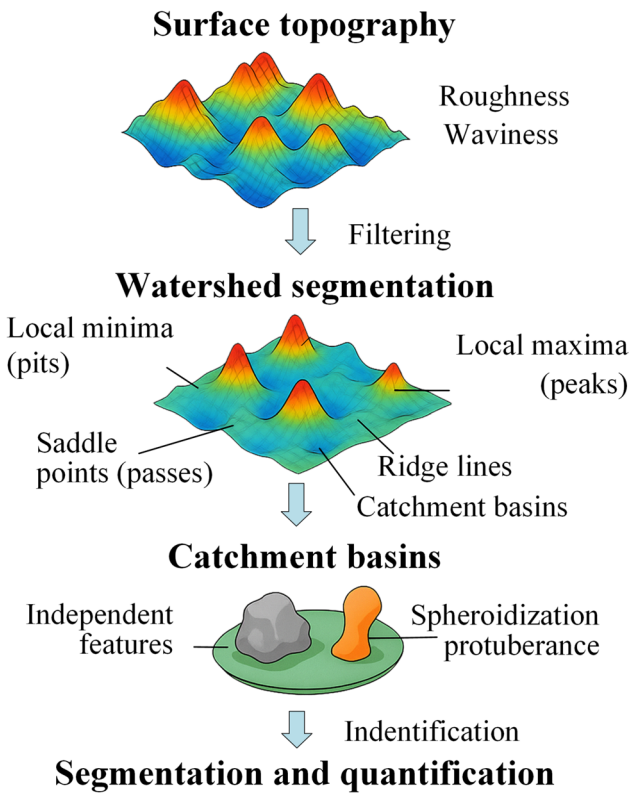


**Fig. 18** Watershed segmentation algorithm

line" (the watershed). Ultimately, the entire surface is partitioned without overlap or omission into "catchment basins" bounded by these ridgelines. Each catchment basin corresponds to an independent feature with a clear topological meaning, such as a pit or a peak [167]. This method has been successfully applied to the analysis of surfaces from metal additive manufacturing (AM), enabling the segmentation and quantification of features that are critical to fatigue performance, such as "unfused powder particles" and "spheroidization protuberances", thereby achieving a leap from "scale characterization" to "functional characterization" [165].

While the watershed algorithm excels at global region partitioning based on gradient flow, it requires the help of the α-shape method from computational geometry to precisely define the geometric attributes of individual, arbitrarily shaped features, especially those with non-convex boundaries [168, 169]. Unlike the global segmentation approach, the α-shape is more focused on accurately extracting the boundary of a single feature from a point cloud [40, 169]. Its mathematical essence is a generalization of the convex hull and is equivalent to a subgraph of the Delaunay triangulation of the point set. Conceptually, it can be understood as using a virtual "disk" of radius α to probe the voids in a point cloud. When α is infinite, the α-shape degenerates to the convex hull. As α decreases, the disk can penetrate deeper into the interior of the point cloud, carving out finer boundaries and even identifying holes. In surface metrology, the morphological α-shape method proposed by Lou et al. [40] combines mathematical morphology operations with the α-shape to robustly identify "peak" and "valley" regions from the surface texture. Its schematic diagram is shown in Fig. 19. Its core advantage is its ability to precisely define the boundaries of non-convex and irregular features. Once the boundary is determined, functionally relevant parameters of the feature, such as volume, area, and curvature, can be accurately calculated.

The watershed algorithm and the α-shape method are complementary: the former is suitable for global region partitioning based on topological gradient flow, while the latter excels at the precise boundary definition of individual

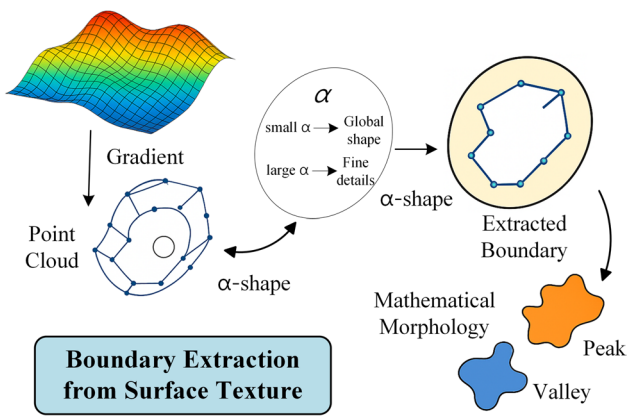


**Fig. 19** Morphological α-shape for boundary extraction

features. They provide a complete toolchain for the quantitative analysis of functional features on freeform surfaces together.

### 5.4 Summary

Freeform surface filtering and analysis techniques revolve around the core scientific problem of "effective multiscale analysis on non-Euclidean manifolds". The theoretical foundation is the geometric flow theory based on the LBO, which provides the mathematical guarantee for intrinsic smoothing. In engineering practice, two main strategies for multiscale decomposition have been developed: algebraic construction and geometric iteration. Through the introduction of watershed segmentation and α-shape methods, a cognitive upgrade from "scale characterization" to the "quantification of functional discrete features" has been achieved. However, these classic methods based on geometric models still have limitations in performance and automation when dealing with extremely complex, highly random surfaces, or when adaptive optimization based on massive data is required. It provides a clear problem orientation and entry point for the data-driven artificial intelligence methods discussed in the next section.

## 6 AI-Driven Surface Filtering

The application of artificial intelligence (AI), particularly machine learning and deep learning, in the field of surface filtering represents not just a performance enhancement but a paradigm-shifting solution to several key problems [170–173]. Traditional filtering algorithms, whether based on frequency-domain analysis or geometric flow, all rely on preset, deterministic mathematical models. However, when faced with complex random textures, unanticipated defects, or the need to mine latent patterns from massive datasets, such methods based on analytical models or fixed rules often reach their theoretical limits [174, 175]. The core value of AI lies in its ability to autonomously learn complex, nonlinear mapping relationships from data, providing a new, data-driven path to address challenges that are difficult for traditional methods to handle, such as complex boundary definition, prediction of data outside boundaries, and interpretation of the correlation between topography and function [176, 177].

### 6.1 Paradigm Shift in Boundary Treatment

In the engineering practice of surface filtering, the precise handling of "boundaries" is a prerequisite for ensuring the validity of the results. This involves two major challenges: accurately identifying the boundaries and eliminating the filtering distortion at the identified boundaries (i.e., the edge effect). AI technology offers an end-to-end solution to these challenges.

Traditional methods rely on local operators such as gradients and thresholds to identify boundaries. In scenarios with low signal-to-noise ratios or complex textures, they are highly prone to confusing true boundaries with noise or rough textures [178]. Deep learning, particularly semantic segmentation techniques based on Fully Convolutional Networks (FCN) [179], provides a paradigm-level solution to this problem [180, 181]. Its core advantage lies in transforming boundary detection from a "signal processing" problem based on local physical quantity changes to an "image understanding" problem that fuses global and local context. Achieving this leap requires a neural network architecture that can balance high-level semantic information (for identifying regional properties) with low-level spatial precision (for delineating exact boundaries). In this context, the U-Net architecture emerged and quickly became the recognized standard in the field [181]. Its symmetric encoder-decoder structure and the signature skip connections enable the network to accurately identify regional attributes by using the global context information provided by the deep network when performing pixel-level precise classification, and to draw clear boundaries with the accurate positioning information of the shallow network, thus resolving the inherent conflict between semantic prediction and precise localization. The BlurRes-UNet model proposed by Cui et al. [182] is a typical application of this architecture in the field of surface metrology, which further enhances the accuracy and robustness of boundary identification by integrating residual learning and a customized loss function.

The edge effect is an inherent problem for all filtering operators based on a finite support window. Its root cause is that when the filter window operates at the data boundary, any algorithm must assume the data outside the boundary. It is difficult for the assumptions made by traditional deterministic extrapolation methods to conform to the true physical characteristics， such as zero-padding or symmetric extension, which inevitably introduce significant signal distortion in the boundary regions [111, 183, 184]. The core idea of machine learning is to shift from "rule-based" deterministic extrapolation to "learning-based" probabilistic inference. Surface extrapolation based on Gaussian Processes (GP) is a prime example of this paradigm shift. Liu et al. [185] utilized Gaussian Processes, a powerful non-parametric Bayesian model, to directly learn the intrinsic spatial correlation of the surface from the data through a covariance function (i.e., a kernel). The process is divided into two steps: (1) in the learning phase, where the GP model is trained using data from within the boundary, allowing it to "learn" the true

texture structure of the surface in that region; and (2) in the inference phase, where the trained model is used to make a posterior prediction (extrapolation) for the region outside the boundary that conforms to the learned statistical laws.

The prediction result is a complete probability distribution, with its mean serving as the most likely extension result. This "intelligently completed" virtual region, which is statistically consistent with the internal data, provides complete data support for subsequent standard filters, thereby eliminating the edge effect at its physical root.

### 6.2 Data Augmentation Based on Generative Models

A common bottleneck in the development and validation of more advanced filtering or functional prediction algorithms is the lack of sufficiently diverse test surfaces with accurate ground truth. The physical preparation and measurement of such surfaces are costly and time-consuming. Generative Adversarial Networks (GANs) [186] provide a revolutionary solution to this problem. Through the adversarial training of a Generator and a Discriminator, GANs can learn the latent distribution of real surface data and then generate statistically equivalent, highly realistic synthetic surface data [48]. These massive and parameter-controllable virtual surfaces can serve as a "digital sandbox" to systematically and efficiently evaluate the performance of different filtering algorithms under various texture conditions, with efficiency and cost-effectiveness far exceeding physical experiments [49].

### 6.3 Physics-Informed Fusion and Explainable Models

While purely data-driven deep learning models have powerful fitting capabilities, their "black box" nature presents a major obstacle to their use in safety-critical engineering applications, where the decision-making process is opaque and the output may violate physical conservation laws [187].

Physics-Informed Neural Networks (PINNs) [188] cleverly fuse the flexibility of data-driven approaches with the rigor of physical models by embedding known physical laws as soft constraints in the form of a regularization term in the neural network's loss function. The core innovation lies in the unique composite loss function structure: $\mathcal{L} = \mathcal{L}_{\text{data}} + \lambda\mathcal{L}_{\text{phys}}$. Here, $\mathcal{L}_{\text{data}}$ is the traditional data-fitting loss, ensuring the model's fidelity to the observed data, while $\mathcal{L}_{\text{phys}}$ is the physics residual loss, which penalizes the network's output for violating known physical equations (typically partial differential equations, PDEs). The key enabling technology for this process is Automatic Differentiation (AD), which can accurately compute the derivatives of the network's output concerning its inputs to any order, thereby allowing physical equations to be directly embedded in the loss function. In the field of surface filtering, Cui et al. [189] significantly improved model performance in small-sample learning scenarios through their research on freeform surface denoising by incorporating physical constraints, such as surface smoothness (represented by curvature continuity), into the loss function. It points to a sophisticated future where the most powerful models will be a deep synthesis of both data-driven and physics-based approaches, resolving the dichotomy between empirical and theoretical models. Additionally, as shown in Fig. 20, an intelligent surface characterization system has been developed to automatically analyze complex surface datasets, extract surface patterns with high accuracy, and quantify key parameters, including field, feature, and functional characteristics [182].

As AI models increasingly become core tools, their interpretability and autonomous decision-making capabilities have become the next hurdle for engineering applications. eXplainable AI (XAI) technologies, represented by SHAP

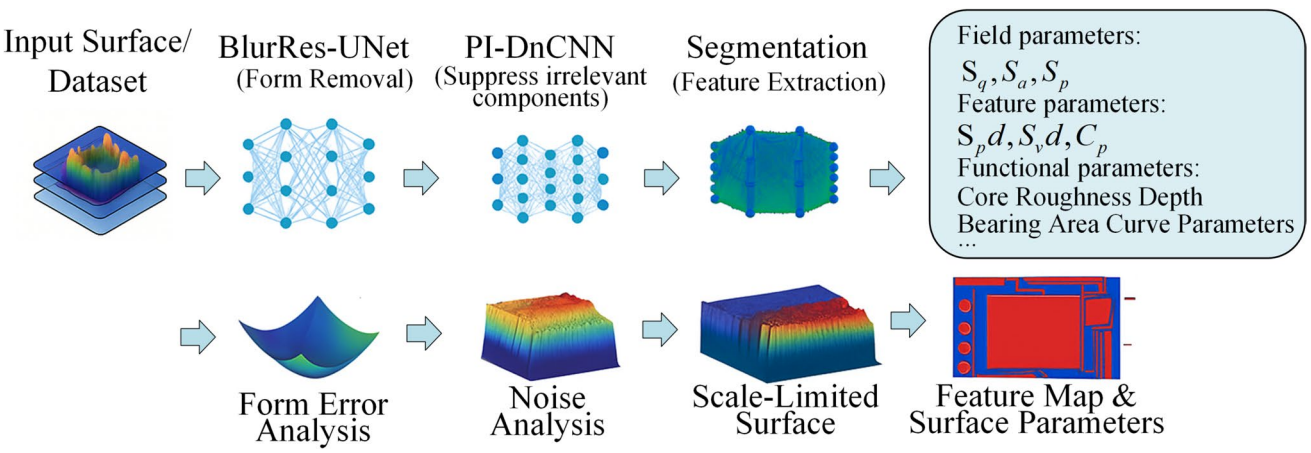


**Fig. 20** Intelligent surface characterization system [182]

and LIME, aim to open the "black box" [106, 190]. SHAP, originating from cooperative game theory, can provide a global analysis of feature importance [191], while LIME explains individual predictions by constructing a local surrogate model [192]. Introducing XAI techniques into the field of surface analysis not only enhances the transparency and trustworthiness of the models but also has the potential to become a new tool for scientific discovery, helping researchers to uncover "process-topography-function" correlation laws that go beyond human experience [193].

### 6.4 Summary

This section has systematically discussed how artificial intelligence provides paradigm-shifting solutions to classic problems in the field of surface filtering. From solving boundary issues with U-Net and Gaussian Processes, to breaking the data bottleneck with GANs, and to enhancing model credibility with PINNs and XAI, AI is fundamentally reshaping the technological landscape of surface analysis. Looking ahead, AI will no longer be merely a post-processing tool but will be deeply integrated with the manufacturing process as a core intelligent decision-making paradigm. It will drive surface engineering toward a more precise, intelligent, and autonomous direction [194].

## 7 Concluding Remarks

### 7.1 Synthesis

Its technological paradigm has undergone a clear transition, moving from an early focus on "signal fidelity" through noise suppression, to a mid-stage emphasis on "geometric fidelity" through feature separation, and now to the current paradigm of "functional perception" guided by intelligent decision-making.

This paper has systematically analyzed the evolutionary trajectory, cutting-edge advancements, and core challenges of engineering surface filtering technology, driven by high-definition metrology. It shows that the development of surface filtering technology profoundly reflects the manufacturing industry's continuous pursuit of functionality, precision, and intelligence. Its technological paradigm has undergone a clear transition, moving from an early focus on "signal fidelity" through noise suppression, to a mid-stage emphasis on "geometric fidelity" through feature separation, and now to the current paradigm of "functional perception" guided by intelligent decision-making.

At the level of technical evolution, a logically clear and comprehensive framework of filtering methods for surfaces of different geometric forms has been established. For continuous flat surfaces, filtering focuses on the fidelity of multiscale signal separation, evolving from standardized methods based on the Gaussian filter to nonlinear multiscale analysis techniques represented by wavelet transform, shearlet transform, and empirical mode decomposition, which enable the fine-grained characterization of anisotropic and non-stationary features. For multi-hole and discontinuous surfaces, filtering has broken through the traditional signal processing paradigm, effectively solving the synergistic problem of boundary preservation and feature separation through strategies of explicit geometric constraints and implicit adaptive decomposition. For freeform surfaces, a complete knowledge system from theory to application has been constructed. Geometric flow theory, with the Laplace-Beltrami Operator (LBO) at its core, has laid the mathematical foundation for intrinsic smoothing. Discrete strategies represented by the lifting wavelet transform and mesh relaxation have enabled engineering implementation, while toolchains centered on watershed segmentation and α-shapes have completed the transition from "scale characterization" to "functional feature quantification".

At the level of paradigm innovation, the deep integration of artificial intelligence is not a simple performance optimization of traditional algorithms but provides a new methodology for solving fundamental bottlenecks in the field. Machine learning-based methods, represented by U-Net semantic segmentation and Gaussian process probabilistic modeling, have completely revolutionized the methods for identifying and handling surface boundaries. Generative Adversarial Networks (GANs) provide an efficient "digital sandbox" for algorithm validation, breaking through the limitations of physical samples. Physics-Informed Neural Networks (PINN) and eXplainable Artificial Intelligence (XAI) directly address the core issues of AI in engineering applications, preliminarily solving the problems of model physical consistency and credibility by embedding physical constraints and enhancing decision transparency.

Despite significant progress, the field still faces multiple challenges. Firstly, when faced with high-definition point cloud data at the billion-point level, the computational efficiency of existing advanced algorithms remains a critical bottleneck that limits their industrial online application. Secondly, a standardized system for evaluating and validating the performance of AI-based filtration methods is absent, hindering the engineering adoption of new technologies. Furthermore, there is a lack of a unified theory for consistent cross-scale feature characterization of hierarchical surfaces that combine macroscopic curvature, microscopic porosity, and micro- to nano-scale textures. Ultimately, the paradigm shifts towards "intelligent functional perception" illuminates that the most profound scientific challenge lies in establishing a universal and precise physical mapping

model between surface topography and functional performance, a core scientific problem that remains to be solved.

### 7.2 Future Work

To address the aforementioned challenges, future research in engineering surface topography filtration technology will focus on the deep integration of advanced data-driven models with physical mechanisms, with the aim of providing more direct scientific guidance for manufacturing and in-service processes. The core development paths are as follows:

Firstly, to construct analytical models with both physical consistency and decision transparency by fusing Physics-Informed Neural Networks (PINN) and eXplainable Artificial Intelligence (XAI). Such models will not only ensure that their analysis results do not violate known physical laws but will also be able to reveal the key features in the surface topography that are decisive for specific functions and their respective weights. It will provide a quantitative and reliable basis for guiding the manufacturing process, such as optimizing cutting parameters to control critical functional textures. Secondly, to develop in-service performance prediction models based on initial topography. For instance, by leveraging the ability of large models such as Transformer to capture long-range dependencies, build evolution prediction models for service behaviors like surface wear and fatigue. Such models can upgrade surface analysis from static characterization to dynamic prediction, for example, by predicting the lifetime decay trend of a sealing surface based on its initial roughness distribution, which can provide forward-looking guidance for equipment life management. Finally, to achieve closed-loop intelligent control of the manufacturing process. Based on reliable "topography-function" mapping and prediction models, in-situ metrology techniques can be integrated with real-time control systems. By extracting key topographical features through online filtering analysis and dynamically adjusting process parameters such as laser power and feed rate, a "measure-analyze-control" closed loop can be formed. This model will fundamentally improve the precision and efficiency of surface quality control, driving the shift of high-performance functional surfaces from "passive inspection" to "active design".

In summary, engineering surface filtering technology is undergoing a paradigm shift. It will no longer be merely a tool for characterizing "as-manufactured topography". Instead, through deep coupling with artificial intelligence, physical mechanisms, and the manufacturing process, it will be upgraded to a core intelligent engine that supports "online quality control" and "performance evolution prediction", providing critical theoretical and technical support for the precise design and controllable manufacturing of high-performance functional surfaces.

**Acknowledgements** This work is supported by National Natural Science Foundation of China (Grant No.52405565, 52275499 and 92467101).

**Author Contributions** Yiping Shao: Investigation, Formal analysis, Methodology, Conceptualization, Supervision, Writing-Original Draft, Review & Editing, Funding acquisition. Zhilong Xu: Investigation, Conceptualization, Literature survey, Formal analysis, Writing-Original Draft, Review & Editing. Shichang Du: Investigation, Formal analysis, Writing-Original Draft, Review & Editing, Funding acquisition, Supervision. Jiansha Lu: Investigation, Writing-Original Draft, Review & Editing.

**Data Availability** The authors declare that all data presented in this article are available.

## Declarations

**Competing interests** The authors have no competing interests to declare that are relevant to the content of this article.

## References

1. Brown, C. A., Hansen, H. N., Jiang, X. J., Blateyron, F., Berglund, J., et al. (2018). Multiscale analyses and characterizations of surface topographies. *CIRP Annals, 67*(2), 839–862. https://doi.org/10.1016/j.cirp.2018.06.001
2. Nam, J., Kim, T., Park, J., Jo, E., Wolf, N., et al. (2024). A study on surface quality and mechanical property improvement through mechanical surface treatment of amorphous metal. *International Journal of Precision Engineering and Manufacturing, 25*(3), 611–616. https://doi.org/10.1007/s12541-023-00919-z
3. He, B., Zheng, H. Y., Ding, S., Yang, R., & Shi, Z. (2023). A review of digital filtering in evaluation of surface roughness. *Metrology and Measurement Systems*. https://doi.org/10.1007/s00454-007-9006-1
4. ASME B46.1. (2019). *Surface Texture (Surface Roughness, Waviness, and Lay)*. The American Society of Mechanical Engineers (ASME).
5. Jiang, X., Senin, N., Scott, P. J., & Blateyron, F. (2021). Feature-based characterisation of surface topography and its application. *CIRP Annals, 70*(2), 681–702. https://doi.org/10.1016/j.cirp.2021.05.001
6. Jacobs, T. D. B., & Pastewka, L. (2022). Surface topography as a material parameter. *MRS Bulletin, 47*(12), 1205–1210. https://doi.org/10.1557/s43577-022-00465-5
7. Yun, D., Gao, Q., Jia, D., & Zhao, B. (2025). Study on milling mechanism and surface roughness of CNTs/2009Al composites. *International Journal of Precision Engineering and Manufacturing, 26*(5), 1061–1073. https://doi.org/10.1007/s12541-024-01169-3
8. Chen, Y., Ding, Y., Zhao, F., Zhang, E., Wu, Z., & Shao, L. J. A. S. (2021). Surface defect detection methods for industrial products: A review. *Applied Sciences, 11*(16), Article 7657. https://doi.org/10.3390/app11167657
9. Lee, H., Kim, J., Guo, X., & Lee, C. (2023). Non-destructive inspection system for self-piercing riveting in CFRP-metal joining product using stereoscopic method with robotic manipulator. *International Journal of Precision Engineering and Manufacturing, 24*(9), 1625–1631. https://doi.org/10.1007/s12541-023-00888-3
10. Park, S.-H., Choi, S., Jhang, K.-Y., & Ha, T. (2023). Nondestructive inspection of directed energy deposited components using

scanning acoustic microscopy with metalworking fluids. *International Journal of Precision Engineering and Manufacturing, 24*(11), 2099–2112. https://doi.org/10.1007/s12541-023-00854-z
11. Tian, G., Yang, C., Lu, X., Wang, Z., Liang, Z., et al. (2023). Inductance-to-Digital Converters (Ldc) Based Integrative Multi-Parameter Eddy Current Testing Sensors for Ndt&E. *NDT & E International, 138*, 102888. https://doi.org/10.1016/j.ndteint.2023.102888
12. Lu, X., Wang, Z., Liang, Z., Peng, F., Yi, Q., & Tian, G. J. (2025). Micro defect detection and characterization using pot-core coils and Ldc. *IEEE Sensors Journal, 25*(8), 13894–13903. https://doi.org/10.1109/JSEN.2025.3547576
13. Bae, D.-S., & Lee, J.-K. (2024). Effect of surface roughness on fatigue strength in martensitic stainless steel. *International Journal of Precision Engineering and Manufacturing, 25*(10), 2125–2131. https://doi.org/10.1007/s12541-024-01079-4
14. Zhang, Q., Wang, B., Song, C., Wang, H., & Shi, Z. (2025). Grinding characteristics and surface roughness modeling of 2.5d woven Sicf/sic ceramic matrix composites. *International Journal of Precision Engineering and Manufacturing, 26*(2), 249–268. https://doi.org/10.1007/s12541-024-01086-5
15. Bons, J. P. (2010). A review of surface roughness effects in gas turbines. *Journal of Turbomachinery-transactions of The Asme, 132*(2), 021004–021019. https://doi.org/10.1115/1.3066315
16. Bonse, J., Kirner, S. V., Höhm, S., Epperlein, N., Spaltmann, D., et al. (2017). Applications of laser-induced periodic surface structures (LIPSS). In *Laser-based Micro-and Nanoprocessing XI*. https://doi.org/10.1117/12.2250919
17. Huang, L., Cao, Y., Peng, R., Li, H., Wang, T., & Wei, G. (2025). Adaptive sampling technique for free-form surface of aero-engine blades based on discrete curvature. *International Journal of Precision Engineering and Manufacturing, 26*(2), 325–344. https://doi.org/10.1007/s12541-024-01161-x
18. Jiang, C.-P., Masrurotin, W., & A. T., Macek, W., & Ramezani, M. (2024). Enhancing internal Cooling Channel Design in Inconel 718 turbine blades via laser powder bed fusion: A comprehensive review of surface topography enhancements. *International Journal of Precision Engineering and Manufacturing, 26*, 487–511. https://doi.org/10.1007/s12541-024-01177-3
19. Ready, J. F. (1997). *Industrial applications of lasers*. Elsevier.
20. Hutter, J. L., & Bechhoefer, J. (1993). Calibration of atomic-force microscope tips. *Review Of Scientific Instruments, 64*(7), 1868–1873. https://doi.org/10.1063/1.1143970
21. Leach, R. (Ed.). (2011). *Optical measurement of surface topography* (Vol. 8). Springer. https://doi.org/10.1007/978-3-642-12012-1
22. De Groot, P. (2015). Principles of interference microscopy for the measurement of surface topography. *Advances in Optics and Photonics, 7*(1), 1–65. https://doi.org/10.1364/AOP.7.000001
23. Zhang, S. (2018). High-speed 3D shape measurement with structured light methods: A review. *Optics and Lasers in Engineering, 106*, 119–131. https://doi.org/10.1016/j.optlaseng.2018.02.017
24. Huang, Z., Shih, A. J., & Ni, J. (2006). Laser Interferometry Hologram Registration for Three-Dimensional Precision Measurements. *Manufacturing Science and Engineering, Parts A and B, 128*(4), 1006–1013. https://doi.org/10.1115/MSEC2006-21104
25. Du, S., & Xi, L. F. (2019). *High definition metrology based surface quality control and applications. Quality Control and Applications*. Springer.
26. Wang, M., Xi, L. F., & Du, S. (2014). 3D surface form error evaluation using high definition metrology. *Precision Engineering, 38*(1), 230–236. https://doi.org/10.1016/j.precisioneng.2013.08.008
27. Li, G., Du, S., Wang, B., Lv, J., & Deng, Y. (2022). High definition metrology-based quality improvement of surface texture in face milling of workpieces with discontinuous surfaces. *Journal of Manufacturing Science and Engineering, 144*(3), Article 031001. https://doi.org/10.1115/1.4051883
28. Fu, S., Muralikrishnan, B., & Raja, J. (2003). Engineering surface analysis with different wavelet bases. *Journal of Manufacturing Science and Engineering, 125*(4), 844–852. https://doi.org/10.1115/1.1616947
29. Podulka, P. (2021). Suppression of the high-frequency errors in surface topography measurements based on comparison of various spline filtering methods. *Materials, 14*(17), Article 14. https://doi.org/10.3390/ma14175096
30. Sherrington, I., & Smith, E. (1986). The significance of surface topography in engineering. *Precision Engineering, 8*(2), 79–87. https://doi.org/10.1016/0141-6359(86)90090-5
31. Townsend, A., Pagani, L., Scott, P. J., & Blunt, L. (2017). Areal surface texture data extraction from X-ray computed tomography reconstructions of metal additively manufactured parts. *Precision Engineering, 48*, 254–264. https://doi.org/10.1016/j.precisioneng.2016.12.008
32. Whitehouse, D. J. (2023). *Handbook of surface metrology*. Routledge.
33. Jiang, X. J., & Whitehouse, D. J. (2012). Technological shifts in surface metrology. *CIRP Annals, 61*(2), 815–836. https://doi.org/10.1016/j.cirp.2012.05.009
34. ISO 16610-1. (2015). Geometrical Product Specifications (GPS)-Filtration—Part 1: Overview and Basic Concepts.
35. Young, I. T., Vliet, L. J., & v. (1995). Recursive implementation of the Gaussian filter. *Signal Process, 44*(2), 139–151. https://doi.org/10.1016/0165-1684(95)00020-E
36. Raja, J., Muralikrishnan, B., & Fu, S. (2002). Recent advances in separation of roughness. *Waviness and Form Precision Engineering, 26*(2), 222–235. https://doi.org/10.1016/S0141-6359(02)00103-4
37. Seewig, J. (2005). Linear and robust Gaussian regression filters. *Journal of Physics: Conference Series, 13*, 254–257. https://doi.org/10.1088/1742-6596/13/1/059
38. Daubechies, I. (1990). The wavelet transform, time-frequency localization and signal analysis. *IEEE Transactions on Information Theory, 36*(5), 961–1005. https://doi.org/10.1109/18.57199
39. Huang, N. E., Shen, Z., Long, S. R., Wu, M. C., Shih, H. H., et al. (1998). The empirical mode decomposition and the hilbert spectrum for nonlinear and non-stationary time series analysis. *Proceedings of the Royal Society of London. Series A: Mathematical, Physical and Engineering Sciences, 454*(1971), 903–995. https://doi.org/10.1098/rspa.1998.0193
40. Lou, S., Jiang, X. J., & Scott, P. J. (2013). Application of the morphological alpha shape method to the extraction of topographical features from engineering surfaces. *Measurement, 46*(2), 1002–1008. https://doi.org/10.1016/j.measurement.2012.09.015
41. Haykin, S. S. (2002). *Adaptive filter theory*. Pearson Education India.
42. Bobenko, A. I., & Springborn, B. A. (2005). A discrete laplace–beltrami operator for simplicial surfaces. *Discrete & Computational Geometry, 38*, 740–756. https://doi.org/10.24425/mms.2021.136606
43. Desbrun, M., Meyer, M., Schröder, P., & Barr, A. H. (1999). Implicit Fairing of Irregular Meshes Using Diffusion and Curvature Flow. In *Proceedings of the 26th Annual Conference on Computer Graphics And Interactive Techniques*. https://doi.org/10.1145/311535.311576
44. Jiang, X., Cooper, P., & Scott, P. J. (2011). Freeform surface filtering using the diffusion equation. *Proceedings of the Royal Society A: Mathematical, Physical and Engineering Sciences, 467*(2127), 841–859. https://doi.org/10.1098/rspa.2010.0307
45. Roy, M., Foufou, S., & Truchetet, F. (2010). Recent advances in multiresolution analysis of 3d meshes and their applications. In *Electronic Imaging*. https://doi.org/10.1117/12.845595

46. Podulka, P., Kulisz, M., & Antosz, K. (2024). Evaluation of high-frequency measurement errors from turned surface topography data using machine learning methods. *Materials, 17*(2), 1456–1462. https://doi.org/10.3390/ma17071456
47. Gu, L., Zhang, L., & Wang, Z. (2021). A one-shot texture-perceiving generative adversarial network for unsupervised surface inspection. In *2021 IEEE iInternational cConference on Image Processing (ICIP)*. https://doi.org/10.1109/ICIP42928.2021.9506202
48. Creswell, A., White, T., Dumoulin, V., Arulkumaran, K., Sengupta, B., & Bharath, A. A. (2018). Generative adversarial networks: An overview. *IEEE Signal Processing Magazine, 35*(1), 53–65. https://doi.org/10.1109/MSP.2017.2765202
49. Kim, T., Kim, J. G., Park, S., Kim, H. S., Kim, N., et al. (2023). Virtual surface morphology generation of Ti-6Al-4V directed energy deposition via conditional generative adversarial network. *Virtual and Physical Prototyping, 18*(1), Article e2124921. https://doi.org/10.1080/17452759.2022.2124921
50. Nguyen, P. C. H., Vlassis, N. N., Bahmani, B., Sun, W., Udaykumar, H. S., & Baek, S. (2022). Synthesizing controlled microstructures of porous media using generative adversarial networks and reinforcement learning. *Scientific Reports, 12*(1), Article 9034. https://doi.org/10.1038/s41598-022-12845-7
51. Barbosa, C. R. H., Sousa, M. C., Almeida, M. F. L., & Calili, R. F. (2022). Smart manufacturing and digitalization of metrology: A systematic literature review and a research agenda. *Sensors (Basel), 22*(16), Article 22. https://doi.org/10.3390/s22166114
52. Wang, R., Law, A. C. C., Garcia, D., Yang, S., & Kong, Z. J. (2021). Development of structured light 3d-scanner with high spatial resolution and its applications for additive manufacturing quality assurance. *International Journal of Advanced Manufacturing Technology, 117*(3–4), 845–862. https://doi.org/10.1007/s00170-021-07780-2
53. Fahrbach, M., Xu, M., Nyang'au, W. O., Domanov, O. A., Schwalb, C. H., et al. (2023). Damped cantilever microprobes for high-speed contact metrology with 3D surface topography. *Sensors, 23*(4), Article 23. https://doi.org/10.3390/s23042003
54. Constantoudis, V., Poulios, K., Chatzigeorgiou, M., & Papavieros, G. (2017). Computational Nanometrology of nanostructures: The challenge of spatial complexity. In *18th International Congress of Metrology.* https://doi.org/10.1051/metrology/201713001
55. Tomovich, S., Peng, Z., Yuan, C., & Yan, X.-p. (2011). Quantitative surface characterisation using laser scanning confocal microscopy. In *Laser Scanning, Theory and Applications* (pp. 1–30). https://doi.org/10.5772/15403
56. Ekberg, P., Su, R., & Leach, R. K. (2017). High-precision lateral distortion measurement and correction in coherence scanning interferometry using an arbitrary surface. *Optics Express, 25*(16), 18703–18712. https://doi.org/10.1364/OE.25.018703
57. Whitehead, S., Shearer, A., Watts, D., & Wilson, N. (1999). Comparison of two stylus methods for measuring surface texture. *Dental Materials, 15*(2), 79–86. https://doi.org/10.1016/S0109-5641(99)00017-2
58. Whitehouse, D. J. (2002). *Handbook of surface and Nanometrology*. Taylor & Francis.
59. Pawlus, P., Reizer, R., & Wieczorowski, M. (2018). Comparison of results of surface texture measurement obtained with stylus methods and optical methods. *Metrology and Measurement Systems, 25*(3), 589–602. https://doi.org/10.24425/123894
60. Stedman, M., & Lindsey, K. (1989). Limits of surface measurement by stylus instruments. In *1988 International Congress on Optical Science and Engineering*. https://doi.org/10.1117/12.949155
61. Cheng, F., Fu, S., & Chen, Z.-Y. (2020). Surface texture measurement on complex geometry using dual-scan positioning strategy. *Applied Sciences, 10*(23), Article 8418. https://doi.org/10.3390/app10238418
62. Giessibl, F. J. (2003). Advances in atomic force microscopy. *Reviews of Modern Physics, 75*(3), 949–983. https://doi.org/10.1103/RevModPhys.75.949
63. Villarrubia, J. S. ((1997)). Algorithms for scanned probe microscope image simulation, surface reconstruction, and tip estimation. *Journal of Research of the National Institute of Standards and Technology, 102*(4), 425–454. https://doi.org/10.6028/jres.102.030
64. Magonov, S. N., & Whangbo, M.-H. (2008). *Surface analysis with Stm and Afm: Experimental and theoretical aspects of image analysis*. John Wiley & Sons.
65. Fang, F., Zhang, X. D., Weckenmann, A., Zhang, G., & Evans, C. J. (2013). Manufacturing and measurement of freeform optics. *CIRP Annals - Manufacturing Technology, 62*(2), 823–846. https://doi.org/10.1016/j.cirp.2013.05.003
66. Jecić, S., & Drvar, N. (2003). The assessment of structured light and laser scanning methods in 3d shape measurements. In *Proceedings of the 4th International Congress of Croatian Society of Mechanics*.
67. Quirrenbach, A. (2001). Optical interferometry. *Annual Review of Astronomy and Astrophysics, 39*(1), 353–401. https://doi.org/10.1146/annurev.astro.39.1.353
68. de Groot, P. J., & de Lega, X. C. (2004). Signal modeling for modern interference microscopes. *Optical Metrology in Production Engineering, 5457*, 26–34. https://doi.org/10.1117/12.546226
69. Nwaneshiudu, A., Kuschal, C., Sakamoto, F. H., Anderson, R. R., Schwarzenberger, K., & Young, R. C. (2012). Introduction to confocal microscopy. *Journal of Investigative Dermatology, 132*(12), 1–5. https://doi.org/10.1038/jid.2012.429
70. Pfeifer, N., & Briese, C. (2007). Laser Scanning–Principles and Applications. In *Geosiberia 2007-International Exhibition and Scientific Congress*.
71. Goodman, J. W. (2007). *Speckle phenomena in optics: Theory and applications*. Roberts and Company Publishers.
72. ISO 16610-31. (2016). Geometrical Product Specifications (GPS)-Filtration—Part 31: Robust Profile Filters: Gaussian Regression Filters.
73. Koide, K., Yokozuka, M., Oishi, S., & Banno, A. (2021). Globally consistent 3D lidar mapping with GPU-accelerated Gicp matching cost factors. *IEEE Robotics and Automation Letters, 6*(4), 8591–8598. https://doi.org/10.1109/LRA.2021.3113043
74. Wu, J., & Zhang, M. (2024). A review of point cloud alignment methods and their applications. *Academic Journal of Science and Technology*. https://doi.org/10.54097/jg0q5p11
75. Podulka, P. (2021). Detection of measurement noise in surface topography analysis. *Journal of Physics: Conference Series, 1736*(1), Article 012014. https://doi.org/10.1088/1742-6596/1736/1/012014
76. Dorsch, R. G., Häusler, G., & Herrmann, J. (1994). Laser triangulation: Fundamental uncertainty in distance measurement. *Applied Optics, 33*(7), 1306–1314. https://doi.org/10.1364/AO.33.001306
77. Ali, S. H. R. (2012). Advanced nanomeasuring techniques for surface characterization. *International Scholarly Research Notices, 2012*, 1–23. https://doi.org/10.5402/2012/859353
78. Armstrong, G., & Kailas, L. W. (2017). Hyphenated analytical techniques for materials characterisation. *European Journal of Physics, 38*(5), Article 3001. https://doi.org/10.1088/1361-6404/aa7e93
79. Silva, M. I., Malitckii, E., Santos, T. G., Vilaça, P. J. P., & i. M. S. (2023). Review of conventional and advanced non-destructive testing techniques for detection and characterization of small-scale defects. *Progress in Materials Science, 138*, 101155. https://doi.org/10.1016/j.pmatsci.2023.101155

80. Marchetti, M., Baria, E., Cicchi, R., & Pavone, F. S. (2019). Custom multiphoton/Raman microscopy setup for imaging and characterization of biological samples. *Methods and Protocols, 2*(2), Article 2. https://doi.org/10.3390/mps2020051
81. Opilik, L., Schmid, T., & Zenobi, R. (2013). Modern raman imaging: Vibrational spectroscopy on the micrometer and nanometer scales. *Annual Review of Analytical Chemistry, 6*(1), 379–398. https://doi.org/10.1146/annurev-anchem-062012-092646
82. Liu, M. Y., Cheung, C. F., Feng, X., Ho, L. T., & Yang, S. M. (2019). Gaussian process machine learning-based surface extrapolation method for improvement of the edge effect in surface filtering. *Measurement, 137*, 214–224. https://doi.org/10.1016/j.measurement.2019.01.048
83. DebRoy, T., Mukherjee, T., Wei, H., Elmer, J., & Milewski, J. (2021). Metallurgy, mechanistic models and machine learning in metal printing. *Nature Reviews Materials, 6*(1), 48–68. https://doi.org/10.1038/s41578-020-00236-1
84. Grasso, M., Remani, A., Dickins, A., Colosimo, B. M., & Leach, R. K. (2021). In-situ measurement and monitoring methods for metal powder bed fusion: An updated review. *Measurement Science and Technology, 32*(11), Article 112001. https://doi.org/10.1088/1361-6501/ac0b6b
85. Kusiak, A. (2018). Smart manufacturing. *International Journal of Production Research, 56*(1–2), 508–517. https://doi.org/10.1080/00207543.2017.1351644
86. Tao, F., Qi, Q., Wang, L., & Nee, A. (2019). Digital twins and cyber–physical systems toward smart manufacturing and industry 4.0: Correlation and comparison. *Engineering, 5*(4), 653–661. https://doi.org/10.1016/j.eng.2019.01.014
87. Uhlemann, T.H.-J., Lehmann, C., & Steinhilper, R. (2017). The digital twin: Realizing the cyber-physical production system for industry 4.0. *Procedia CIRP, 61*, 335–340. https://doi.org/10.1016/j.procir.2016.11.152
88. Leach, R., Haitjema, H., Su, R., & Thompson, A. (2020). Metrological characteristics for the calibration of surface topography measuring instruments: A review. *Measurement Science and Technology, 32*(3), Article 032001. https://doi.org/10.1088/1361-6501/abb54f
89. Gröger, S., Dietzsch, M., Gerlach, M., & Jess, S. (2005). `Real mechanical profile' — The new approach for nano-measurements. *Journal of Physics: Conference Series*. https://doi.org/10.1088/1742-6596/13/1/004
90. Osanna, P. H. (1979). Surface roughness and size tolerance. *Wear, 57*(2), 227–236. https://doi.org/10.1016/0043-1648(79)90097-8
91. Velazquez, S. R., Nguyen, T. Q., & Broadstone, S. R. (1998). Design of hybrid filter banks for analog/digital conversion. *IEEE Transactions on Signal Processing, 46*(4), 956–967. https://doi.org/10.1109/78.668549
92. Cooley, J. W., & Tukey, J. W. (1965). An algorithm for the machine calculation of complex Fourier series. *Mathematics of Computation, 19*(90), 297–301. https://doi.org/10.1090/S0025-5718-1965-0178586-1
93. Singleton, R. C. (1969). An algorithm for computing the mixed radix fast Fourier transform. *IEEE Transactions on Audio and Electroacoustics, 17*(2), 93–103. https://doi.org/10.1109/TAU.1969.1162042
94. ISO 11562. (1996). Geometrical product specifications (GPS)-surface texture: Profile method—Metrological characteristics of phase correct filters.
95. Unser, M., Aldroubi, A., & Eden, M. (1993). B-spline signal processing. I. Theory. *IEEE Transactions on Signal Processing, 41*(2), 821–833. https://doi.org/10.1109/78.193220
96. Barak, P. (1995). Smoothing and differentiation by an adaptive-degree polynomial filter. *Analytical Chemistry, 67*(17), 2758–2762. https://doi.org/10.1021/ac00113a006
97. Scott, P., & Jiang, X. (2014). Freeform surface characterisation: Theory and practice. *Journal of Physics: Conference Series*. https://doi.org/10.1088/1742-6596/483/1/012005
98. ISO 16610-41. (2015). Geometrical Product Specifications (GPS)-Filtration—Part 41: Morphological Profile Filters: Disk and Horizontal Line-Segment Filters.
99. Thakur, R. S., Chatterjee, S. J., Yadav, R. N., & Gupta, L. (2021). Image de-noising with machine learning: A review. *IEEE Access, 9*, 93338–93363. https://doi.org/10.1109/ACCESS.2021.3092425
100. Sorkine-Hornung, O. (2005). Laplacian mesh processing. *Eurographics*. https://doi.org/10.2312/egst.20051044
101. Ronneberger, O., Fischer, P., & Brox, T. (2015). U-net: Convolutional networks for biomedical image segmentation. In *Medical image computing and computer-assisted intervention – MICCAI 2015* https://doi.org/10.1007/978-3-319-24574-4_28
102. Zhang, Z., Liu, Q., & Wang, Y. (2018). Road extraction by deep residual U-net. *IEEE Geoscience and Remote Sensing Letters, 15*(5), 749–753. https://doi.org/10.1109/LGRS.2018.2802944
103. Hartung, J., Dold, P. M., Jahn, A., & Heizmann, M. (2022). Analysis of AI-based single-view 3d reconstruction methods for an industrial application. *Sensors (Basel), 22*(17), Article 22. https://doi.org/10.3390/s22176425
104. Sun, J., & Jiang, A. (2024). Automation of design innovation process based on cad technology and reinforcement learning. *Computer-Aided Design and Applications*, 84–99. https://doi.org/10.14733/cadaps.2024.S23.84-99
105. Karniadakis, G. E., Kevrekidis, I. G., Lu, L., Perdikaris, P., Wang, S., & Yang, L. (2021). Physics-informed machine learning. *Nature Reviews Physics, 3*(6), 422–440. https://doi.org/10.1038/s42254-021-00314-5
106. Molnar, C. (2020). *Interpretable machine learning*. *Lulu. com*.
107. Shao, Y., Wang, K., Du, S., & Xi, L. (2018). High definition metrology enabled three dimensional discontinuous surface filtering by extended tetrolet transform. *Journal of Manufacturing Systems, 49*, 75–92. https://doi.org/10.1016/j.jmsy.2018.09.002
108. Li, W., Xin, Q., Fan, B., Chen, Q., & Deng, Y. (2024). A review of emerging technologies in ultra-smooth surface processing for optical components. *Micromachines, 15*(2), Article 15. https://doi.org/10.3390/mi15020178
109. Chen, X., Raja, J., & Simanapalli, S. (1995). Multi-scale analysis of engineering surfaces. *International Journal of Machine Tools and Manufacture, 35*(2), 231–238. https://doi.org/10.1016/0890-6955(94)P2377-R
110. Tong, M., Zhang, H., Ott, D., Chu, W., & Song, J. (2015). Applications of the spline filter for areal filtration. *Measurement Science and Technology, 26*(12), Article 127002. https://doi.org/10.1088/0957-0233/26/12/127002
111. Janecki, D. (2011). Gaussian filters with profile extrapolation. *Precision Engineering, 35*(4), 602–606. https://doi.org/10.1016/j.precisioneng.2011.04.003
112. Krystek, M. (1996). Form filtering by splines. *Measurement, 18*(1), 9–15. https://doi.org/10.1016/0263-2241(96)00039-5
113. Brinkmann, S., Bodschwinna, H., & Lemke, H.-W. (2001). Accessing roughness in three-dimensions using Gaussian regression filtering. *International Journal of Machine Tools and Manufacture, 41*(13–14), 2153–2161. https://doi.org/10.1016/S0890-6955(01)00082-7
114. Serra, J. P. F. (1987). Image analysis and mathematical. *Morphology*. https://doi.org/10.1109/TPAMI.1987.4767941
115. Soille, P. (1999). *Morphological image analysis: Principles and applications* (Vol. 2). *Springer*.
116. Jiang, X. J., Lou, S., & Scott, P. J. (2011). Morphological method for surface metrology and dimensional metrology based on the alpha shape. *Measurement Science and Technology, 23*(1), Article 015003. https://doi.org/10.1088/0957-0233/23/1/015003

117. Wang, Y., Liu, Y., Zhang, G., Guo, F., Liu, X.-f, & Wang, Y. (2018). Extraction of features for surface topography by morphological component analysis. *Tribology International, 123*, 191–199. https://doi.org/10.1016/j.triboint.2018.03.001
118. Zhang, D. (2019). Wavelet Transform. In *Fundamentals of image data mining: Analysis, features, classification and retrieval* (pp. 35–44). Springer.
119. Valette, S., & Prost, R. (2004). Wavelet-based multiresolution analysis of irregular surface meshes. *EEE Transactions on Visualization and Computer Graphics, 10*(2), 113–122. https://doi.org/10.1109/TVCG.2004.1260763
120. Wang, Y.-P., Lee, S. L., & Toraichi, K. (1999). Multiscale curvature-based shape representation using B-spline wavelets. *IEEE Transactions on Image Processing: A Publication of the IEEE Signal Processing Society, 8*(11), 1586–1592. https://doi.org/10.1109/83.799886
121. Du, S., Liu, C., & Huang, D. (2015). A shearlet-based separation method of 3D engineering surface using high definition metrology. *Precision Engineering, 40*, 55–73. https://doi.org/10.1016/j.precisioneng.2014.10.004
122. Flandrin, P., Rilling, G., & Goncalves, P. (2004). Empirical mode decomposition as a filter bank. *IEEE Signal Processing Letters, 11*(2), 112–114. https://doi.org/10.1109/LSP.2003.821662
123. Zeiler, A., Faltermeier, R., Keck, I. R., Tomé, A. M., Puntonet, C. G., & Lang, E. W. (2010). Empirical mode decomposition-an introduction. In *2010 international joint conference on neural networks (IJCNN)*. https://doi.org/10.1109/IJCNN.2010.5596829
124. Deléchelle, E., Lemoine, J., & Niang, O. (2005). Empirical mode decomposition: An analytical approach for sifting process. *IEEE Signal Processing Letters, 12*(11), 764–767. https://doi.org/10.1109/LSP.2005.856878
125. Du, S., Liu, T., Huang, D., & Li, G. (2018). A fast and adaptive bi-dimensional empirical mode decomposition approach for filtering of workpiece surfaces using high definition metrology. *Journal of Manufacturing Systems, 46*, 247–263. https://doi.org/10.1016/j.jmsy.2018.01.005
126. Tatone, B. S., & Grasselli, G. (2013). An investigation of discontinuity roughness scale dependency using high-resolution surface measurements. *Rock Mechanics and Rock Engineering, 46*(4), 657–681. https://doi.org/10.1007/s00603-012-0294-2
127. Wang, M., Shao, Y.-P., Du, S.-C., & Xi, L.-f. (2015). A diffusion filter for discontinuous surface measured by high definition metrology. *International Journal of Precision Engineering and Manufacturing, 16*(10), 2057–2062. https://doi.org/10.1007/s12541-015-0267-y
128. Perona, P., & Malik, J. (2002). Scale-space and edge detection using anisotropic diffusion. *IEEE Transactions on Pattern Analysis and Machine Intelligence, 12*(7), 629–639. https://doi.org/10.1109/34.56205
129. Kass, M., Witkin, A., & Terzopoulos, D. (1988). Snakes: Active contour models. *International Journal of Computer Vision, 1*(4), 321–331. https://doi.org/10.1007/BF00133570
130. Mallat, S. G. (2002). A theory for multiresolution signal decomposition: The wavelet representation. *IEEE Transactions on Pattern Analysis and Machine Intelligence, 11*(7), 674–693. https://doi.org/10.1109/34.192463
131. Weickert, J. (1998). *Anisotropic diffusion in image processing* (Vol. 1).
132. Krommweh, J. (2010). Tetrolet transform: A new adaptive Haar wavelet algorithm for sparse image representation. *Journal of Visual Communication and Image Representation, 21*(4), 364–374. https://doi.org/10.1016/j.jvcir.2010.02.011
133. Schmid, P. J., & Ecole, P. (2010). Dynamic mode decomposition of numerical and experimental data. *Journal of Fluid Mechanics, 656*, 5–28. https://doi.org/10.1017/S0022112010001217
134. Cohen, A., Daubechies, I., & Feauveau, J. C. (1992). Biorthogonal bases of compactly supported wavelets. *Communications on Pure and Applied Mathematics, 45*(5), 485–560. https://doi.org/10.1002/cpa.3160450502
135. Strela, V., & Walden, A. (1998). *Signal and image Denoising via wavelet Thresholding: Orthogonal and biorthogonal, scalar and multiple wavelet transforms* (pp. 124–157). *Nonlinear and Non-stationary Signal Processing*.
136. Rilling, G., Flandrin, P., & Goncalves, P. (2003). On empirical mode decomposition and its algorithms. In *IEEE-EURASIP workshop on nonlinear signal and image processing NSIP-03*.
137. Wu, Z., & Huang, N. E. (2009). Ensemble empirical mode decomposition: A noise-assisted data analysis method. *Advances in Adaptive Data Analysis, 1*(1), 1–41. https://doi.org/10.1142/S1793536909000047
138. Gilles, J. (2013). Empirical wavelet transform. *IEEE Transactions on Signal Processing, 61*(16), 3999–4010. https://doi.org/10.1109/TSP.2013.2265222
139. Gilles, J., Tran, G., & Osher, S. (2014). 2D empirical transforms. Wavelets, ridgelets, and curvelets revisited. *SIAM Journal on Imaging Sciences, 7*(1), 157–186. https://doi.org/10.1137/130923774
140. Shao, Y., Du, S., & Tang, H. (2021). An extended bi-dimensional empirical wavelet transform based filtering approach for engineering surface separation using high definition metrology. *Measurement, 178*, Article 109259. https://doi.org/10.1016/j.measurement.2021.109259
141. Pitard, G., Le Goïc, G., Favreliere, H., Samper, S., Desage, S.-F., & Pillet, M. (2015). Discrete modal decomposition for surface appearance modelling and rendering. In *IEEE-EURASIP workshop on nonlinear signal and image processing NSIP-03*.
142. Rowley, C. W., Mezić, I., Bagheri, S., Schlatter, P., & Henningson, D. S. (2009). Spectral analysis of nonlinear flows. *Journal of Fluid Mechanics, 641*, 115–127. https://doi.org/10.1017/S0022112009992059
143. Shao, Y., Xu, F., Chen, J., Lu, J., & Du, S. (2023). Engineering surface topography analysis using an extended discrete modal decomposition. *Journal of Manufacturing Processes, 90*, 367–390. https://doi.org/10.1016/j.jmapro.2023.02.005
144. Jiang, X., & P. S., D. Whitehouse. (2017). Freeform surface characterisation - a fresh strategy. *CIRP Annals, 56*(1), 553–556. https://doi.org/10.1016/j.cirp.2007.05.132
145. Kumar, S., Tong, Z., & Jiang, X. J. (2022). Advances in the design and manufacturing of novel freeform optics. *International Journal of Extreme Manufacturing, 4*(3), Article 032004. https://doi.org/10.1088/2631-7990/ac7617
146. Bala Muralikrishnan, J. R. (2009). *Computational surface and roundness metrology*. Springer.
147. Morimoto, T. ((1993)). Geometric structures on filtered manifolds. *Hokkaido Mathematical Journal, 22*(3), 263–347. https://doi.org/10.14492/hokmj/1381413178
148. Reuter, M., Wolter, F.-E., & Peinecke, N. (2006). Laplace–Beltrami Spectra as 'Shape-Dna'of Surfaces and Solids. *Computer-Aided Design, 38*(4), 342–366. https://doi.org/10.1016/j.cad.2005.10.011
149. Bunge, A., Herholz, P., Kazhdan, M., & Botsch, M. (2020). Polygon laplacian made simple. *Computer Graphics Forum*. https://doi.org/10.1111/cgf.13931
150. Taubin, G. (1995). A Signal Processing Approach to Fair Surface Design. In *Proceedings of the 22nd Annual Conference on Computer Graphics and Interactive Techniques*. https://doi.org/10.1145/218380.218473
151. Clarenz, U., Diewald, U., & Rumpf, M. (2000). Anisotropic Geometric Diffusion in Surface Processing. Proceedings Visualization 2000. VIS 2000 (Cat. No.00CH37145). https://doi.org/10.1109/VISUAL.2000.885721.

152. Bao, J., Jing, J., Zhang, W., Liu, C., & Gao, T. (2022). A corner detection method based on adaptive multi-directional anisotropic diffusion. *Multimedia Tools and Applications, 81*(20), 28729–28754. https://doi.org/10.1007/s11042-022-12666-w
153. Botsch, M., Kobbelt, L., Pauly, M., Alliez, P., & Lévy, B. (2010). *Polygon mesh processing*. CRC Press.
154. Dong, S., Bremer, P.-T., Garland, M., Pascucci, V., & Hart, J. C. (2006). Spectral surface Quadrangulation. In *SIGGRAPH '06: ACM SIGGRAPH 2006 papers*. https://doi.org/10.1145/1179352.11419
155. Lounsbery, M., DeRose, T. D., & Warren, J. (1997). Multiresolution analysis for surfaces of arbitrary topological type. *Acm Transactions on Graphics, 16*(1), 34–73. https://doi.org/10.1145/237748.237750
156. Wang, P.-S., Liu, Y., & Tong, X. (2016). Mesh denoising via cascaded normal regression. *Acm Transactions On Graphics, 35*, 1–12. https://doi.org/10.1145/2980179.2980232
157. Liu, T., Chen, M., Song, Y., Li, H., & Lu, B. (2017). Quality improvement of surface triangular mesh using a modified laplacian smoothing approach avoiding intersection. *PLoS One, 12*(9), Article e0184206. https://doi.org/10.1371/journal.pone.0184206
158. Sweldens, W. (1998). The lifting scheme: A construction of second generation wavelets. *SIAM Journal on Mathematical Analysis, 29*(2), 511–546. https://doi.org/10.1137/S0036141095289051
159. Chen, H., Xu, W., Broderick, N., & Han, J. (2018). An adaptive denoising method for Raman spectroscopy based on lifting wavelet transform. *Journal of Raman Spectroscopy, 49*(9), 1529–1539. https://doi.org/10.1002/jrs.5399
160. Jiang, X., Abdul-Rahman, H. S., & Scott, P. J. (2013). Multi-scale freeform surface texture filtering using a mesh relaxation scheme. *Measurement Science and Technology, 24*(11), Article 115001. https://doi.org/10.1088/0957-0233/24/11/115001
161. Xu, S., Fang, J., & Li, X. (2019). Weighted Laplacian method and its theoretical applications. *IOP Conference Series: Materials Science and Engineering, 768*(7), 07203. https://doi.org/10.1088/1757-899X/768/7/072032
162. ISO 25178-2. (2021). Geometrical product specifications (GPS)-surface texture: Areal—Part 2: Terms. *Definitions and Surface Texture Parameters*.
163. Vincent, L., & Soille, P. (1991). Watersheds in digital spaces: An efficient algorithm based on immersion simulations. *IEEE Transactions on Pattern Analysis & Machine Intelligence, 13*(6), 583–598. https://doi.org/10.1109/34.87344
164. Bieniek, A., & Moga, A. (2000). An efficient watershed algorithm based on connected components. *Pattern Recognition, 33*(6), 907–916. https://doi.org/10.1016/S0031-3203(99)00154-5
165. Lou, S., Pagani, L., Zeng, W., Jiang, X. J., & Scott, P. J. (2020). Watershed segmentation of topographical features on freeform surfaces and its application to additively manufactured surfaces. *Precision Engineering, 63*, 177–186. https://doi.org/10.1016/j.precisioneng.2020.02.005
166. Delgado-Friedrichs, O., Robins, V., & Sheppard, A. (2014). Skeletonization and partitioning of digital images using discrete Morse theory. *IEEE Transactions on Pattern Analysis and Machine Intelligence, 37*(3), 654–666. https://doi.org/10.1109/TPAMI.2014.2346172
167. Scoville, N. A. (2019). *Discrete Morse theory* (Vol. 90). American Mathematical Soc.
168. Guo, B., Menon, J., & Willette, B. (1997). Surface reconstruction using alpha shapes. *Computer Graphics Forum*. https://doi.org/10.1111/1467-8659.00178
169. Edelsbrunner, H., & Mücke, E. P. (1994). Three-dimensional alpha shapes. *ACM Transactions on Graphics, 13*(1), 43–72. https://doi.org/10.1145/174462.156635
170. LeCun, Y., Bengio, Y., & Hinton, G. (2015). Deep learning. *Nature, 521*(7553), 436–444. https://doi.org/10.1038/nature14539
171. Butler, K. T., Davies, D. W., Cartwright, H., Isayev, O., & Walsh, A. (2018). Machine learning for molecular and materials science. *Nature, 559*(7715), 547–555. https://doi.org/10.1038/s41586-018-0337-2
172. Feng, H., Liu, J., van Ostayen, R., Ji, C., & Xu, H. (2025). Integration of machine learning prediction and optimization for determination of the coefficient of friction of textured Uhmwpe surfaces. *Proceedings of the Institution of Mechanical Engineers, Part J: Journal of Engineering Tribology, 239*(2), 173–188. https://doi.org/10.1177/13506501241272816
173. Alzubaidi, L., Zhang, J., Humaidi, A. J., Al-dujaili, A., Duan, Y., et al. (2021). Review of deep learning: Concepts, Cnn architectures, challenges, applications. *Future Directions Journal of Big Data, 8*. https://doi.org/10.1186/s40537-021-00444-8
174. Sharp, N., Attaiki, S., Crane, K., & Ovsjanikov, M. (2020). Diffusionnet: Discretization agnostic learning on surfaces. *ACM Transactions on Graphics (TOG), 41*(3), 1–16. https://doi.org/10.1145/3414685.3417839
175. Sharp, N., & Crane, K. (2020). You can find geodesic paths in triangle meshes by just flipping edges. *Acm Transactions On Graphics, 39*(6), 1–15. https://doi.org/10.1145/3414685.3417839
176. Duan, C., Chen, S., & Kovacevic, J. (2019). 3d Point Cloud Denoising Via Deep Neural Network Based Local Surface Estimation. In *ICASSP 2019–2019 IEEE international conference on acoustics, Speech and Signal Processing (ICASSP)*. https://doi.org/10.1109/ICASSP.2019.8682812
177. Mukherjee, S., Kottayil, N. K., Sun, X., & Cheng, I. (2019). Cnn-based real-time parameter tuning for optimizing Denoising filter performance. In *International Conference on Image Analysis and Recognition*. https://doi.org/10.1007/978-3-030-27202-9_10
178. Canny, J. (1986). A computational approach to edge detection. *IEEE Transactions on Pattern Analysis and Machine Intelligence, 8*(6), 679–698. https://doi.org/10.1109/TPAMI.1986.4767851
179. Long, J., Shelhamer, E., & Darrell, T. (2015). Fully convolutional networks for semantic segmentation. In *Proceedings of the IEEE Conference on Computer Vision and Pattern Recognition*. https://doi.org/10.1109/CVPR.2015.7298965
180. Garcia-Garcia, A., Orts-Escolano, S., Oprea, S., Villena-Martinez, V., & Garcia-Rodriguez, J. (2017). A review on deep learning techniques applied to semantic segmentation. arXiv,1704.06857. https://doi.org/10.48550/arXiv.1704.06857
181. Minaee, S., Boykov, Y., Porikli, F., Plaza, A., Kehtarnavaz, N., & Terzopoulos, D. (2021). Image segmentation using deep learning: A survey. *IEEE Transactions on Pattern Analysis and Machine Intelligence, 44*(7), 3523–3542. https://doi.org/10.1109/TPAMI.2021.3059968
182. Cui, W., Lou, S., Zeng, W., Kadirkamanathan, V., Qin, Y., et al. (2025). Blurres-Unet: A novel neural network for automated surface characterisation in metrology. *Computers in Industry, 165*, Article 104228. https://doi.org/10.1016/j.compind.2024.104228
183. Oppenheim, A. V. (1999). *Discrete-Time Signal Processing*. Pearson Education India.
184. ISO 16610-21. (2012). Geometrical Product Specifications (GPS)-Filtration Part—21: Linear Profile Filters: Gaussian Filters.
185. Binois, M., & Wycoff, N. (2021). A survey on high-dimensional Gaussian process modeling with application to Bayesian optimization. *ACM Transactions on Evolutionary Learning and Optimization, 2*(2), 1–26. https://doi.org/10.1145/3545611
186. Goodfellow, I. J., Pouget-Abadie, J., Mirza, M., Xu, B., Warde-Farley, D., et al. (2021). Generative adversarial networks. In *2023*

*14th international conference on computing communication and networking technologies (ICCCNT)*. https://doi.org/10.1109/ICCCNT56998.2023.10306417
187. Kim, D., & Lee, J. (2024). A review of physics informed neural networks for multiscale analysis and inverse problems. *Multiscale Science and Engineering, 6*(1), 1–11. https://doi.org/10.1007/s42493-024-00106-w
188. Raissi, M., Perdikaris, P., & Karniadakis, G. E. (2019). Physics-informed neural networks: A deep learning framework for solving forward and inverse problems involving nonlinear partial differential equations. *Journal Of Computational Physics, 378*, 686–707. https://doi.org/10.1016/j.jcp.2018.10.045
189. Cui, W., Lou, S., Zeng, W., Kadirkamanathan, V., Qin, Y., et al. (2024). Unlocking freeform structured surface denoising with small sample learning: Enhancing performance via physics-informed loss and detail-driven data augmentation. *Advanced Engineering Informatics, 62*, Article 102733. https://doi.org/10.1016/j.aei.2024.102733
190. Salih, A. M. A., Raisi-Estabragh, Z., Galazzo, I. B., Radeva, P., Petersen, S. E., et al. (2025). A perspective on explainable artificial intelligence methods: Shap and Lime. *Advanced Intelligent Systems, 7*(1), 2400304. https://doi.org/10.1002/aisy.202400304
191. Lundberg, S. M., & Lee, S.-I. (2017). *A unified approach to interpreting model predictions*. *Advances In Neural Information Processing Systems*.
192. Ribeiro, M. T., Singh, S., & Guestrin, C. (2016). "Why Should I Trust You?" Explaining the Predictions of Any Classifier. In *Proceedings of The 22nd ACM SIGKDD International Conference on Knowledge Discovery and Data Mining*.
193. Mishra, A., Jatti, V. S., Sefene, E. M., & Paliwal, S. (2023). Explainable artificial intelligence (Xai) and supervised machine learning-based algorithms for prediction of surface roughness of additively manufactured polylactic acid (Pla) specimens. *Applied Mechanics, 4*(2), 668–698. https://doi.org/10.3390/applmech4020034
194. Pantić, M., Jovanović, S., Djordjevic, A., Petrović Savić, S., Radenković, M., & Šarkoćević, Ž. (2025). Predicting wear rate and friction coefficient of Li2si2o5 dental ceramic using optimized artificial neural networks. *Applied Sciences, 15*(4), Article 1789. https://doi.org/10.3390/app15041789



**Yi-ping Shao** received the B.E. degree in industrial engineering from the Beijing Institute of Technology, Beijing, China, in 2014, and the Ph.D. degree in mechanical engineering from Shanghai Jiao Tong University, Shanghai, China, in 2020. He is currently an Assistant Professor with the College of Mechanical Engineering, Zhejiang University of Technology. His current research interests include intelligent manufacturing, measurement and quality control. He serves as a member of the Early Career Advisory Board for the journal Measurement.

**Zhilong Xu** received the B.E. degree in industrial engineering from the Zhejiang university of Technology, Hangzhou, China, in 2022, and has been pursuing a PhD degree at the College of Mechanical Engineering of Zhejiang University of Technology since 2022. His current research interests include intelligent manufacturing, measurement, quality control, machine learning, intelligent logistics.

**Shichang Du** (Member, IEEE) received the B.S. and M.S.E. degrees in mechanical engineering from the Hefei University of Technology, Hefei, China, in 2000 and 2003, respectively, and the Ph.D. degree in industrial engineering and management from Shanghai Jiao Tong University (SJTU), Shanghai, China, in 2008. He was with the University of Michigan, Ann Arbor, MI, USA, from 2006 to 2007, as a Visiting Scholar. He is currently a Professor with the Department of Industrial Engineering and Management, Shanghai Jiao Tong University. He has authored/coauthored 100 articles in journals, including IEEE TIM, IEEE TASE, ASME Transaction and IISE Transaction, etc. His current research interests focus on quality control and smart manufacturing methods. His research has been supported by the National Natural Science Foundation of China, the Ministry of Science and Technology of China, and the Shanghai Association for Science and Technology. He receives various awards for his research and teaching, including IEEE TASE Googol Best New Application Paper Award, QR2MSE Best Paper Award, and Most Popular Professor Award of ME School in SJTU. He serves for several journals an Area Editor including Computers and Industrial Engineering, Flexible Services and Manufacturing Journal, Precision Engineering, International Journal of Precision Engineering and Manufacturing, Measurement, Journal of Intelligent Manufacturing, and Computers in Industry.

**Jiansha Lu** received the M.S. degree in Zhejiang University, Hangzhou, China, in 1996. He is currently a Professor with the College of Mechanical Engineering, Zhejiang University of Technology, Hangzhou, China. His current research interests include intelligent manufacturing, intelligent logistics and lean production.